Interaction Notes

Note 518

March 1996

Methodology and Models for Estimating HPM Responses Conducted into a Protective Enclosure

F. M. Tesche
~~EM~~ Consultant
Dallas, TX
72461.3170@Compuserve.com

Abstract

Past studies of the penetration of EM energy into a shielded system have been hampered by a lack of adequate coupling and penetration models, as well as by uncertainties in many of the parameters which define the problem geometry and electrical configuration. This note suggests a methodology for estimating the internal responses of a system, together with an estimate of the importance of the various problem parameters.

The report is divided into two parts. Part 1 summarizes an analysis technique that may be used for electrically complex systems. This is based on the topological view of the system and permits the development of an interaction sequence diagram in the usual manner. The response at a particular observation point is viewed as a function of the many parameters of the problem. Suitable partial derivatives of the response are taken numerically to define the response elasticities—quantities that provide a measure of the importance of the various parameters on determining the total response. In addition, a Monte Carlo computational scheme is suggested for determining the statistical nature of the system responses, due to uncertainties in the system parameters.

Part 2 illustrates this suggested methodology by considering a simple hypothetical system model. The elements of the model that are used are discussed and justifications for using transmission line theory at high frequencies is offered. Typical results are presented to illustrate the responses of the system to a lumped transient voltage source excitation on a line entering the shielded building.

Interaction Notes

Note 518

August 1996

Methodology and Models for Estimating HPM Responses Conducted into a Protective Enclosure

F. M. Tesche
EMC Consultant
Dallas, TX
72461.3170@Compuserve.com

Abstract

Past studies of the penetration of EM energy into a shielded system have been hampered by a lack of adequate coupling and penetration models, as well as by uncertainties in many of the parameters which define the problem geometry and electrical configuration. This note suggests a methodology for estimating the internal responses of a system, together with an estimate of the importance of the various problem parameters.

The note is divided into two parts. Part 1 summarizes an analysis technique that may be used for electrically complex systems. This is based on the topological view of the system and permits the development of an interaction sequence diagram in the usual manner. . The response at a particular observation point is viewed as a function of the many parameters of the problem. Suitable partial derivatives of the response are taken numerically to define the response elasticities—quantities that provide a measure of the importance of the various parameters on determining the total response. In addition, a Monte Carlo computational scheme is suggested for determining the statistical nature of the system responses, due to uncertainties in the system parameters.

Part 2 illustrates this suggested methodology by considering a simple hypothetical system model. The elements of the model that are used are discussed and justifications for using transmission line theory at high frequencies is offered. Typical results are presented to illustrate the responses of the system to a lumped transient voltage source excitation on a line entering the shielded building.

TABLE OF CONTENTS

TABLE OF CONTENTS 2

LIST OF FIGURES 4

ACKNOWLEDGMENT 5

PART 1

ANALYSIS TECHNIQUES FOR ELECTRICALLY COMPLEX SYSTEMS

1. INTRODUCTION 6

2. TRADITIONAL ANALYSIS METHODOLOGY 7

2.1 TOPOLOGICAL CONCEPTS 7
2.1.1 Topological Diagram 7
2.1.2 Interaction Sequence Diagram 8
2.1.3 System Model 8
2.1.4 Circuit Model 9
2.2 ANALYSIS TECHNIQUES 9
2.3 NEEDED MODELING IMPROVEMENTS 10

3. SENSITIVITY ANALYSIS OF SYSTEM-LEVEL RESPONSES 11

3.1 OVERALL CONCEPT 11
3.2 RESPONSE SCALARS 11
3.3 ELASTICITIES 12
3.4 WAVEFORM DEVIATIONS 13

4. STATISTICAL REPRESENTATION OF SYSTEM RESPONSES 14

4.1 REPRESENTATION OF PARAMETER VARIATION 14
4.2 MONTE CARLO SIMULATION 16
4.3 NORM RESPONSES 16
4.3.1 Probability Density Functions *16*
4.3.2 Cumulative Probability Distribution *18*
4.4 DISCUSSION 18

PART 2

ELECTRICAL MODEL FOR HPM ENERGY PENETRATION INTO A SHIELDED ENCLOSURE

5. INTRODUCTION 19

6. PROBLEM DESCRIPTION 19

6.1 GEOMETRY 19
6.2 TOPOLOGY DIAGRAM 20

6.3 INTERACTION SEQUENCE DIAGRAM 21
6.4 SYSTEM MODEL 21
6.5 CIRCUIT DIAGRAM 22

7. MODELING DETAILS 24

7.1 THE TRANSMISSION LINE MODEL 24
7.1.1 The External Line Parallel to the Groundplane 26
7.1.2 The Vertical Transmission Line Section 28
7.1.3 The Coaxial Line 29

8. COMPUTED RESPONSES 30

8.1 SYSTEM RESPONSES 32
8.1.1 Baseline Responses 32
8.1.2 Elasticities 33
8.1.3 Difference Waveforms 34
8.2 STATISTICAL RESPONSES 36
8.2.1 Probability Density Functions 36
8.2.2 Cumulative Probability Distribution 39

9. SUMMARY AND OBSERVATIONS 41

LIST OF FIGURES

Figure 1. Illustration of the normal probability distribution of a variable with a mean value of $\mu = 2$ and a standard deviation $\sigma = 0.2$. 15
Figure 2. Computational procedure for Monte Carlo simulation of system responses. 17
Figure 3. Problem geometry. 20
Figure 4. System topology. 20
Figure 5. The interaction sequence diagram 21
Figure 6. A transmission line model for the interaction path. 22
Figure 7. Circuit model for the transmission line network. 23
Figure 8. Representation of a single transmission line section by an equivalent Thévenin circuit. 24
Figure 9. Analysis procedure for calculating the load response for the network in Figure 7. 25
Figure 10. Comparison of the characteristic impedance for a line with h = 1m and a = 0. 5 cm for the high frequency (scattering) model and the low frequency (transmission line model). 27
Figure 11. Comparison of the characteristic impedances of Figure 10 at higher frequencies. 27
Figure 12. Example of the input impedance for a line with L = 5 m, h = 1 m, a = 0.5 cm and termination impedance of 100 Ω for the two different analyses. 28
Figure 13. Excitation waveform $V_S(t)$ for sample calculation. 31
Figure 14. Spectral magnitude of the damped sine excitation function. 31
Figure 15. Transient load voltage at the internal load. 32
Figure 16. Comparison of the load voltage spectrum and the excitation spectrum. 33
Figure 17. Elasticities for the scalar parameters. 34
Figure 18. Plot of the difference in the load voltage response for a 1% change in the value of the external line length, L_1. 35
Figure 19. Plot of the difference in the load voltage response for a 1% change in the value of h_2. 35
Figure 20. Plot of the difference in the load voltage response for a 1% change in the value of the internal line radius, a_{b1}. 36
Figure 21. Probability density function for the peak negative load voltage. 37
Figure 22. Probability density function for the peak positive load voltage. 38
Figure 23. Probability density function for the energy delivered to the load. 38
Figure 24. Cumulative probability distribution for the peak negative load voltage. 39
Figure 25. Cumulative probability distribution for the peak positive load voltage. 40
Figure 26. Cumulative probability distribution for the energy delivered to the load. 40

ACKNOWLEDGMENT

This work was supported by the Phillips Laboratory, under a subcontract from Kaman Sciences Corp. Thanks are due to Dr. Robert L. Gardner of the Phillips Laboratory, and Donald P. McLemore for their support and technical discussions during this project.

PART 1

ANALYSIS TECHNIQUES FOR ELECTRICALLY COMPLEX SYSTEMS

1. INTRODUCTION

For mission-critical or otherwise sensitive systems, it is frequently necessary to know its possible responses to external electromagnetic (EM) excitations. Such EM stresses can occur from natural lightning, man-made electromagnetic interference (EMI) sources, nuclear electromagnetic pulses (NEMP) arising from a nuclear detonation, or from high-power microwave (HPM) sources. The knowledge of the system response to this stress is useful in performing assessments on the system, in developing hardening measures if needed, and in providing information and knowledge for future system development.

For highly complex systems, such as an aircraft or a ground-based communications facility, the most reliable method for evaluating system responses is by testing. In this manner, the actual EM environment (or a suitably simulated environment) is applied to the system and the responses of interest are noted. Given the relatively large expense involved in system-level testing, however, a common alternative for estimating system responses is to use analytical and numerical methods. While these models are inherently limited in their accuracy, they do provide the flexibility of performing sensitivity studies and statistical calculations that are usually not possible with experiments. Thus, even though analytical models are inexact, they provide very useful information and are frequently used.

This note discusses some of the modeling techniques that may be applied to electrically large and complex systems. Part 1 of the note concentrates on aspects of the overall modeling, which is based on the concept of electromagnetic topology. In this discussion, alternate ways of calculating and viewing system responses are suggested.

In Part 2 of this note, the modeling concepts detailed in Part 1 are applied to a simple example involving conducting wire penetrations into a shielded enclosure, or building. In this example, a fast-rise external EM stress is considered, and as a result, there is a significant high-frequency content in the excitation spectrum. The implications of this on the internal coupling model are discussed.

2. TRADITIONAL ANALYSIS METHODOLOGY

The analysis of electrically large systems presents a true challenge, not only because of the complexity of the system, but also because of the different ways that EM energy can interact with the system, including the mechanisms of inductive and capacitive coupling, EM radiation, current and charge propagation on conductors, aperture penetrations, diffusion through imperfect conductors and cavity-mode resonances.

Early attempts at developing analysis models for such systems were hampered by not having a structures way of decomposing the system into smaller, simpler parts. This led to models with errors frequently exceeding 30 dB when compared with experimental results[1]. In an attempt to decrease these errors, investigators realized that for many types of systems, there may be several layers of conducting surfaces which shield the interior. Known as the "onion" concept of shielding[2], this idea was refined by Baum[3] and Tesche[4], and later formalized in the literature[5,6].

2.1 TOPOLOGICAL CONCEPTS

The idea behind the topological decomposition of a system is really quite simple: the system is examined for the principal shields or EM "barriers" that keep the energy from entering the system. Various imperfections in these shields are noted and categorized. On this basis, a signal flow diagram is constructed and an analysis of the behavior of EM signals propagating along this signal pathway is performed to estimate the internal responses. The elements of this procedure are summarized below, with a concrete example of these concepts being deferred until Part 2.

2.1.1 Topological Diagram

The first step in the model development is determining the topological diagram of the system. This is a description of the principal shielding surfaces in the system and their interrelations with each other. Usually, the choice of the shielding surfaces is evident, as

---

[1] Carter, J. M., and W. L. Curtis, "Common Mode Model Development for Complex Cable Systems", Boeing Company, AFWL-TR-74-60, 1974.

[2] Ricketts, L. W., J. E. Bridges and J. Miletta, *EMP Radiation and Protective Techniques*, John Wiley and Sons, New York, 1976.

[3] Baum, C. E., "How to Think About EMP Interaction", *Proceedings of the 1974 Spring FULMEN Meeting*, Kirtland AFB, April 1974.

[4] Tesche, F. M., et. al., "Internal Interaction Analysis: Topological Concepts and Needed Model Improvements", Interaction Note Series, IN-248, October 1975.

[5] Tesche, F. M., "Topological Concepts for Internal EMP Interaction," *IEEE Trans. AP*, Vol. AP-26, No. 1, January 1978.

[6] Baum, C. E., "Electromagnetic Topology for the Analysis and Design of Complex Electromagnetic Systems", pp. 467-547 in *Fast Electrical and Optical Measurements*, Vol I, eds. I.E. Thompson and L.H. Luessem, Martinus Nijhoff, Dordrecht, 1986.

in the case of an aircraft, where the outer skin forms the first barrier. Other times, however, the shielding barrier becomes difficult to "see" physically, but it exists nevertheless. An example is when two antennas are orientated perpendicularly so that there is no interaction between the two[7]. This leads to the concept of a "virtual" shield, as discussed by Karlsson[8].

If the EM barriers comprising the topological shields were perfect, there would be no energy entering to the system. However, real shields are not perfect, and the EM energy can enter by one or more of the following mechanisms:

- hard-wired penetrations, formed by wires, cables or other conductors,
- aperture penetrations through holes in the shield, and
- diffusion through the barrier material.

These types of points of entry (POE) must be identified in each of the topological surfaces for use in developing the interaction sequence diagram.

2.1.2 Interaction Sequence Diagram

The interaction sequence diagram represents the paths that the external EM energy can take from the outside to the inside of the system. Thus, it is like a signal flow diagram developed from the topological diagram and the POEs, and in a sense, forms a diagram that is the dual of the topological diagram.

In the most rigorous sense, the energy flow along such a pathway is bi-directional. This implies that there can be mutual coupling between the interior and exterior regions of the system. For systems that are designed to be hardened, however, this coupling becomes very small, and the energy propagation may be treated as flowing only in one direction: from the outside to the system interior. This greatly simplifies the analysis, in that the computational models needed to describe this propagation are relatively simple.

2.1.3 System Model

With the interaction sequence diagram developed, it is possible to formulate an appropriate system model for conducting the analysis. This model can be thought of as resulting from the removal of all of the unimportant "clutter" in the system, keeping only the important pieces of the system that pertain to the energy penetration or propagation along the defined pathways.

This step in the analysis can require considerable judgment on the part of the analyst. Eliminating an important piece of the EM problem may contribute to large modeling errors. Keeping in too much detail, however, can make the analysis untenable.

---

[7] Vance, E. F., and W. Graf, "The Role of Shielding in Interference Control", *IEEE Trans. EMC*, Vol. 30, No.3, August, 1988.

[8] Karlsson, T. "The Topological Concept of a Generalized Shield," AFWL Interaction Note 461, Kirtland AFB NM, January 1988.

2.1.4 Circuit Model

Once the system model is developed, it is usually desired to compute the response induced at some component or other electrical load within the system. This is done by reducing, or collapsing, the system model into an equivalent Thévenin or Norton circuit which can be applied to the load. Thus, the entire system interaction model is put into the form of a single circuit. Of course, the elements of this circuit usually are not known analytically—they must be calculated using one or more computer programs, which provide numerical representations of the circuits.

2.2 ANALYSIS TECHNIQUES

Using the topological approach, analysis of various systems to external EM environments has been conducted[9,10,11]. Initial skepticism[12] about the feasibility of using this method for accurate calculations has been dispelled by the recent work of Parmantier[13,14], where very good correspondence between theoretical and experimental results has been noted.

Key to obtaining good theoretical results in this case is the use of an accurate transmission line model for computing EM energy propagation in a system. Using system topology as a starting point, the BLT equation was developed by Baum, Liu, and Tesche for the analysis of energy propagation on a network of multiconductor transmission lines[15]. This analysis procedure resulted in the first multiconductor network code, QV7TA, which permitted lumped or EM-field excitation of the network[16]. Extensions of this work have led to the CRIPTE code presently in use by the Parmantier group in France.

---

[9] Tesche, F. M, et. al., "Application of Topological Methods for Electromagnetic Hardening of the MX Horizontal Shelter System", LuTech, Inc. report prepared for Air Force Weapons Laboratory and Mission Research Corporation under Contract F29601-78-C-0082, January 1981.

[10] Tesche, F. M., et. al., "Summary of Application of Topological Shielding Concepts to Various Aerospace Systems", LuTech, Inc. report prepared for Air Force Weapons Laboratory and Mission Research Corporation under Contract F29601-78-C-0082, February 1981

[11] Tesche, F.M., "Introduction to Concepts of Electromagnetic Topology as Applied to EMP Interaction With Systems", NATO/AGARD Lecture Series Publication 144, *Interaction Between EMP, Lightning and Static Electricity with Aircraft and Missile Avionics Systems*, May 1986.

[12] Longmire, C. L., private communication with the author, Mission Research Corp., 1980.

[13] Parmantier, J. P., V. Gobin, and F. Issac, "Application of EM Topology on Complex Systems", *Proceedings of the 1993 IEEE EMC Symposium*, Dallas, TX. August 1993.

[14] Parmantier, J. P., et. al. "An Application of the Electromagnetic Topology Theory to the EMPTAC Test-Bed Aircraft", Proceedings of the 6th FULMEN Meeting, Phillips Laboratory, November 29, 1993.

[15] Baum C. E., F. M. Tesche, and T.K. Liu "On the Analysis of General Multiconductor Transmission Line Networks", EMP Interaction Notes, Note 350, November 1978.

[16] Tesche, F. M, and T. K. Liu, "User Manual and Code Description for QV7TA: A General Multiconductor Transmission Line Analysis Code", LuTech, Inc., prepared under AFWL contract F29601-78-C-0002, August 1978.

2.3 NEEDED MODELING IMPROVEMENTS

Notwithstanding the previous success in modeling provided by the topological concepts and the BLT equation, there are some deficiencies in the analysis that need to be remedied —especially in the way that calculations are performed. Typically, the analysis models require the definition of an excitation field (usually in the form of a transient waveform), and the choice of an observation quantity useful for quantifying the system behavior to the excitation. An example would be the induced voltage at an electrical component inside the system. Applying one of the many computational models for the system[17] result in a knowledge of the transient voltage waveform at this component. Although a significant amount of effort has gone into getting such a response, there is little information gained as a result. Unanswered are the following questions:

- how typical is the response?
- what are the maximum and minimum values of the response?
- if parameters defining the system change slightly, how much does the response change?
- how accurate is the response?

Answers to these questions cannot be found in the single waveform analysis described above. However, by modifying the analysis concepts as proposed in the following sections, some of these questions can be addressed.

[17] Tesche, F. M., M. Ianoz, and T. Karlsson, *EMC Analysis Methods and Computational Models*, John Wiley and Sons, New York, in press.

3. SENSITIVITY ANALYSIS OF SYSTEM-LEVEL RESPONSES

3.1 OVERALL CONCEPT

The first suggested change in the modeling philosophy is to perform a sensitivity analysis for the problem, instead of simply computing the transient responses at observation locations. In all problems, there are errors in determining the parameters defining the geometry, electrical constants, or other data. These uncertainties arise from measurement errors, random variations in the parameters, or sometimes simply because the measured data are not available and guesses (engineering judgment) are used.

A computational model, developed from the BLT equation for example, is deterministic, in the sense that it always gives the same result for the same input. However, it can be used in several different ways to obtain more information about the computed result. Consider the case of a simple function $f(x)$, where x is some independent variable. The derivative of f, $df(x)/dx$, can be used to quantify the rate of change of the function for any given x. The larger the value of the derivative, the more sensitive is the function to slight variations in the value of x. In a similar manner, a calculated response of a system, say a transient voltage waveform $v(t)$, can be thought of as actually being a function of all of the parameters in the model: $v(x_1,x_2,x_3,...x_n;t)$. These parameters, denoted by x_n, may represent quantities like the line length, wire radius, aperture size—anything that goes into describing the model.

As in the case of the single function, the sensitivity of the voltage v to changes in the various parameters is defined by the n partial derivatives

$$v_n' = \frac{\partial v}{\partial x_n}. \qquad (1)$$

which can be easily computed from the model by using a finite-difference approach involving a total of n+1 calculations.

3.2 RESPONSE SCALARS

Notice that the observable quantity used here for illustration is a transient waveform. It is possible to define one or more scalar quantities, sometimes called norms, to represent and understand this response[18]. Possible norms include the energy contained in the response, the peak values (both positive and negative) of the response, and the maximum rate of rise of the waveform. These are useful, because the large amount of transient data can be combined into several scalar numbers representing the system behavior.

---

[18] Baum, C. E., "Norms and Eigenvector Norms", *Mathematics Notes*, Note 63, November 1979.

In the study to be conducted in Part 2, three scalar quantities are used. These are the load energy and the peak positive and negative values of the waveform. Assuming a purely resistive load, these are defined as

$$E = \int_{-\infty}^{\infty} v(t)i(t)dt = \frac{1}{R_L}\int_{-\infty}^{\infty} v^2(t)dt \tag{2a}$$

$$V_{max} = Max[V(t)] \text{ and } V_{min} = Min[V(t)] \tag{2b}$$

3.3 ELASTICITIES

The response scalars, derived from the transient response, can be used by themselves to describe the system. However, the *change* in these numbers with respect to changes in the system parameters is also of interest, and this can provide significant information about system sensitivities. One possible way of representing this information is to simply calculate the rates of change of the scalars with respect to all n parameters as in Eq.(1). Thus, for the energy, there are n partial derivatives

$$E_i' = \frac{\partial E}{\partial x_i} \quad (i = 1,2,\ldots n). \tag{3}$$

For extremely simple models, these indicated partial derivatives can be can be determined analytically. However, for more complicated systems, a numerical evaluation is needed.

One drawback of using the partial derivatives in Eq.(3) for sensitivity studies is that it is possible to have a case in which one particular partial derivative has a large value corresponding to a very sensitive variable, but its contribution to the overall response can be very small. Thus, to put these partial derivatives in proper perspective, it is possible to define the *elasticity* $\mathcal{E}$ of the energy with respect to the various n parameters as[19]

$$\mathcal{E}(E)_i = \frac{\partial E / \partial x_i}{E / x_i}. \tag{4}$$

Elasticities can be defined for the other scalar observables, as well.

These elasticities provide a convenient way for characterizing the relative importance of the parameters in determining the overall response. A zero value of $\mathcal{E}_i$ for variable x_i indicates that it plays a negligible role in determining the total response. Consequently, it is not necessary to know (i.e., to measure) this value accurately. A large value of $\mathcal{E}_i$, however, signifies a significant variable and suggests that its value must be known accurately.

Furthermore, these elasticities provide guidance as to which parameters should be controlled or otherwise modified in order to more efficiently reduce the internal response (i.e., to harden the system.)

3.4 WAVEFORM DEVIATIONS

Another potentially useful way of characterizing the importance of variations or uncertainties in the parameters of the problem is to consider differences in waveform responses. Consider a particular parameter x_i undergoing a change Δx_i. From Eq.(1), the corresponding change in the voltage waveform is given as

$$\Delta v(t) = \frac{\partial v(t)}{\partial x_n} \Delta x_i \tag{5}$$

which amounts to a time-dependent difference waveform.

The amplitudes of these waveforms illustrate the relative importance of the variations of each of parameters. More important, however, is that they also provide information about the *time of arrival* of the effects from these parameters. As a result, they can be very useful in characterizing the system.

---

[19] Thomas, G. B., *Calculus and Analytic Geometry*, Fourth ed., Addison-Wesley, Reading Mass, 1968,. p 255.

4. STATISTICAL REPRESENTATION OF SYSTEM RESPONSES

The proceeding discussion has examined one way of assessing the importance of individual parameters on a system response. It is also of interest to know the variation of the *total* response as all of the parameters of the problem vary in some prescribed manner. This leads to a statistical representation of the system.

Such an idea is certainly not new. Morgan[20] has discussed statistical ideas pertaining to random variations in multiconductor transmission lines, and Graham[21] has treated random loops and wires in an attempt to better understand EM coupling in systems. This approach, however, does not seem to have been widely used in system-level EM studies involving transient excitations. This section of the note will briefly discuss a statistical method of calculation, involving many repetitive evaluations of the model to generate the appropriate probability functions for the responses.

4.1 REPRESENTATION OF PARAMETER VARIATION

The first step in doing this is to be able to represent the random variations of a particular parameter in a suitable manner. This can be done by developing a probability density function (PDF) which provides the probability of finding a particular value of the variable. While the only way of determining such a distribution is by making repeated observations of the parameter and presenting the resulting values as a histogram, there are several "standard" analytical expressions for approximating these distributions. One common distribution is the normal, or Gaussian, distribution which has the form

$$P(x) = \frac{1}{\sigma\sqrt{2\pi}} e^{-\frac{1}{2}\left(\frac{x-\mu}{\sigma}\right)^2}, \qquad (6)$$

where μ represents the mean value of distribution and σ is the standard deviation. In this manner, any variable in the problem can be represented by a pair of two real numbers, with the actual value of the parameter occurring at random with a probability given by Eq.(6).

Given a specific pair of parameters (μ, σ), a mapping of the random deviates generated from a *uniform* probability distribution (as obtained from a standard random number generator in the interval [0 - 1]) can be made to provide random deviates having the normal probability distribution of Eq.(6). As discussed by Press[22], a randomly selected value of the parameter x is given by the expression

---

[20] Morgan, M. A. and F. M. Tesche, "Basic Statistical Concepts for Analysis of Random Cable Coupling Problems," *IEEE Trans. AP*, Vol. AP-26, No. 1, January 1978.

[21] Graham, W. R., and T. C. Mo, "Probability Distribution of CW Induced currents on Randomly Oriented Subresonant Loops and Wires", *IEEE Trans. AP*, Vol. AP-26, No. 1, January 1978.

[22] Press, W. H., et. a., *Numerical Recipes*, Cambridge Press, New York, 1866, p. 203.

$$x = \mu + y_1 \sigma \sqrt{-2 \frac{\ln(y_1^2 + y_2^2)}{(y_1^2 + y_2^2)}} \qquad (7)$$

where y_1 and y_2 are both independent, randomly chosen variables between -1 and 1. These latter variables may be expressed in terms of random deviates in the interval [0-1], which are denoted by z_1 and z_2, as

$$y_1 = 2 z_1 - 1 \quad \text{and} \quad y_1 = 2 z_1 - 1. \qquad (8)$$

These latter numbers are easily generated using a random number generator.

As an example, Figure 1 illustrates the probability distribution function for a variable x having a mean value of $\mu = 2$ and a standard deviation $\sigma = 0.2$. The solid line represents the analytical distribution function and the thin line is the result of 10,000 random samples.

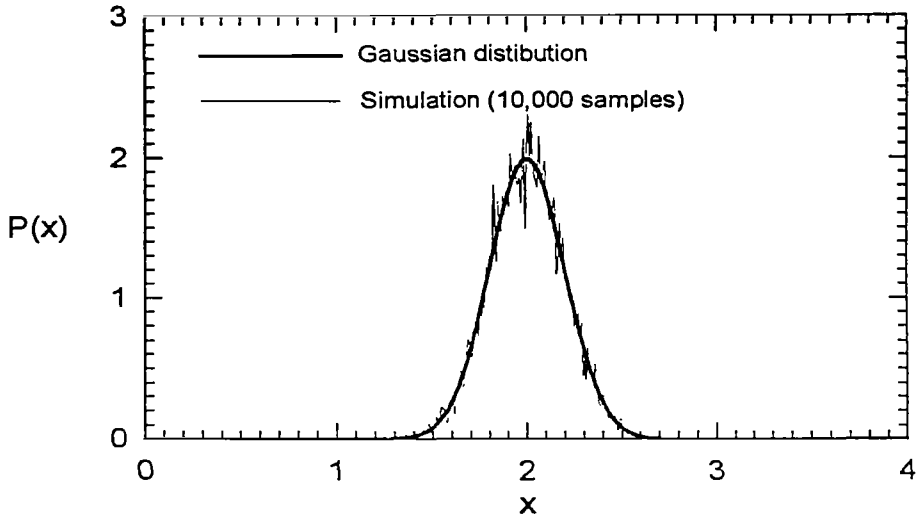

Figure 1. Illustration of the normal probability distribution of a variable with a mean value of $\mu = 2$ and a standard deviation $\sigma = 0.2$.

In representing parameters of a complex system problem in this manner, there are several issues to consider. First and foremost is the question as to whether the Gaussian distribution is really appropriate for representing the data. As noted in Figure 1, the distribution function is symmetric about the mean value, and in some circumstances, this can lead to unphysical values being selected. For example, a variable with a small μ and a large σ could result in a *negative* value of x being generated. If x represented the radius of a wire, say, this would be unphysical and indicates that the distribution is not the correct one for the problem.

A second consideration is that there are interrelations between the various parameters of a problem. For example, in the case of a wire of radius a and height h

parallel to and above a ground plane, it is always required that $h \geq a$. Clearly, if values of h and a are chosen at random, there may be instances in which this condition is not met and the resulting geometry is unphysical. Such cases need to be identified and eliminated in any calculation.

4.2 MONTE CARLO SIMULATION

Once a method of generating random values of the parameters of a particular problem has been developed, it is a simple matter to perform a series of calculations using the deterministic analysis procedure to evaluate the probability distribution functions for specified responses in the system. This Monte Carlo approach is quite simple, although it may require a very large number of calculations—especially if there are a large number of independent parameters in the problem.

Figure 2 illustrates the computational procedure for the Monte Carlo simulation. From a practical standpoint, it is important to realize that the iterative loop may involve a significant amount of computer time, during which there may be a computer interruption due to a power failure, processor "glitch", or other occurrence. Thus, it is important to write the computed result at the end of each iteration in an *append* mode to a data file, so that not all of the data are lost in the event of a failure.

4.3 NORM RESPONSES

For the Monte Carlo simulation, the calculated results are the various scalar quantities that have been discussed earlier. As the calculations proceed, each of these variables are stored on disk, and when the required calculations have been completed, these data are sorted into bins according to their values. Typically, several hundred bins may be used, each of which will then contain an integer number representing the number of times that the calculated result occurred with the value represented by the bin width. This raw binned data can then be used to develop the probability density function and the cumulative probability function for the data.

4.3.1 Probability Density Functions

For a *continuous* function, the distribution of a variable x is described in terms of a frequency function $N(x)$, such that $N(x)dx$ represents the number of times that the variable takes on the particular value x. The probability density function (PDF) of x is defined in terms of N as

$$P(x) = \frac{N(x)}{\int_{-\infty}^{\infty} N(x)dx} \quad , \tag{9}$$

where the integral serves to suitably normalize the function. In this manner, the quantity $P(x)dx$ represents the probability that the parameter takes on the particular value x.

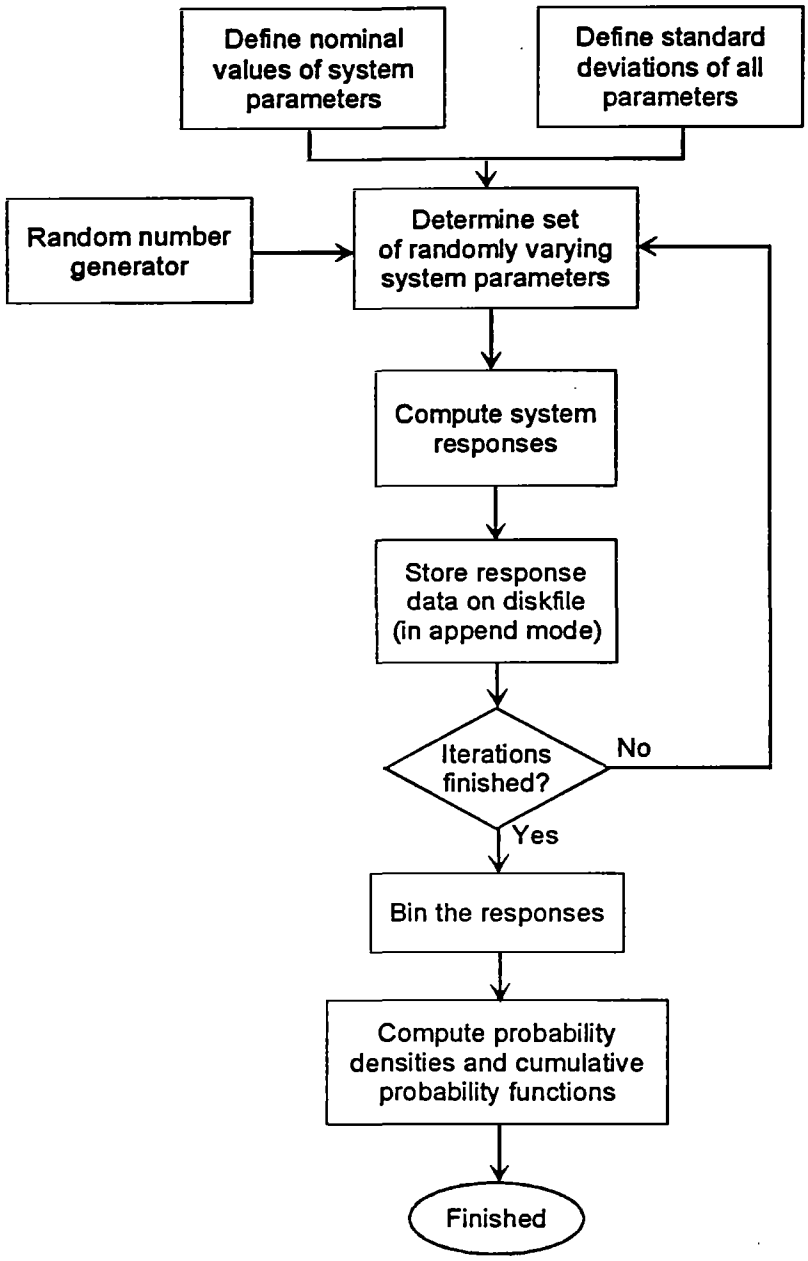

Figure 2. Computational procedure for Monte Carlo simulation of system responses.

The PDF for a discretely sampled function, like the binned data discussed above, is represented by the discrete integer function $N(x_i)$, where x_i is the midpoint value of each bin and the bin width is Δx_i,. The discrete PDF is given as in a manner similar to Eq.(9) as

$$P(x_i) = \frac{N(x_i)}{\sum_k N(x_k)\Delta x_i} \quad i = 1,2..\text{nbins} \ . \tag{10}$$

As we take the data computed from the Monte Carlo simulation and put it into discrete bins, it is this latter equation that is used to compute the PDF for the selected observables.

4.3.2 Cumulative Probability Distribution

Another way of presenting exactly the same information contained in the PDF is to use the cumulative probability distribution (CPD), denoted by $\mathcal{C}$. This quantity is simply the running integral of the PDF, and as a consequence, it appears as a much smoother function.

This function is defined as

$$\mathcal{C}(x) = \int_{-\infty}^{x} P(\xi)d\xi = \frac{\int_{-\infty}^{x} N(\xi)d\xi}{\int_{-\infty}^{\infty} N(\xi)d\xi} \tag{11}$$

and physically, it denotes the probability that the parameter being described will take on the value of *x or less*. Consequently, for very small values of x the value of $\mathcal{C}$ is small, and as x increases, $\mathcal{C}$ increases and eventually reaches the probability of 1.

Another related function is the complementary CPD, $\mathcal{C}_c$, which is evaluated as

$$\mathcal{C}_c(x) = 1 - \mathcal{C}(x). \tag{12}$$

This function represents the probability that the parameter in question will take on the value of *x or more*, and consequently, at small values of x it is unity, and it drops to zero for large values of x. Frequently, the distinction between these two functions is not made clear, and both are referred to as *the* cumulative probability distribution. In this event, it should be immediately evident from the nature of the function what it is representing.

4.4 DISCUSSION

This section of the note has reviewed some basic statistical tools that can be used to understand the behavior of an electrically complex system through computational models. A Monte Carlo simulation of the expected responses has been outlined, and a way of determining the importance of various parameters in the system was suggested. In the next part of this note, these concepts are illustrated using a particular example—that of a shielded building with EM energy entering on a conducting path, such as a power or signal cable.

PART 2

ELECTRICAL MODEL FOR HPM ENERGY PENETRATION INTO A SHIELDED ENCLOSURE

5. INTRODUCTION

As an example of the use of the various calculational techniques suggested in the previous part of this note, we will consider the re-distribution of externally-produced EM energy within a shielded enclosure. As will be noted shortly, the most general version of this problem can be very complex, due to the many different penetration and propagation mechanisms can exist in the real system. In this problem, however, we will consider only the propagation and re-distribution of energy along a single-wire pathway in the form of a tree network. This clearly is a subset of the complete problem, but the goal here is not to perform a complete analysis, but to illustrate the overall computational philosophy and to discuss some of the modeling concepts.

As mentioned in part 1, the key to modeling this type of problem is in the development of a topological diagram and interaction sequence diagram for the system. This will be discussed in the following section.

6. PROBLEM DESCRIPTION

6.1 GEOMETRY

The geometry treated in this analysis consists of a long external line leading into a building, as shown in Figure 3. An example of such a conductor is the electrical power line or telephone cable. The line passes through a weatherhead connection at the top of a vertically oriented conduit and then enters into a circuit breaker/distribution box located inside the building. At this point, the cable fans out into several different internal lines, each containing an electrical load at the end.

In this model, we assume that the external line #1 extends to infinity away from the building, and that the excitation of the network is provided by a localized voltage source, V_S, on this line. The responses to this source are determined at the load impedance located at the end of one of the internal lines.

Note that this problem involves only a single conductor network Realistic power or communication lines usually have multiple conductors, and as a consequence, their responses can be considerably different from those predicted here, due to the existence of both common and differential modes on the lines. In the present analysis, only the common mode responses are estimated for such multiconductor lines

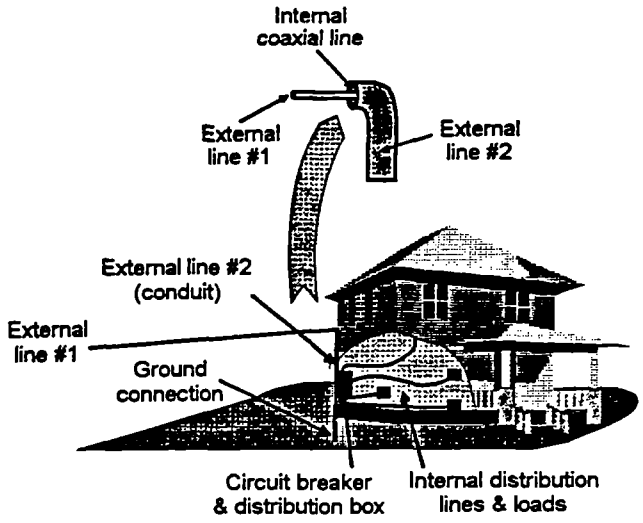

Figure 3. Problem geometry.

6.2 TOPOLOGY DIAGRAM

The key to modeling this problem is the use of topological shielding concepts In this manner, the system can be thought of as consisting of several shielding surfaces or "barriers", which attenuate the external EM energy. In the simple system model treated here, the EM energy is assumed to enter the building only along the conducting paths formed by wires. In a more general problem, there will be aperture and diffusive penetrations, as well, but these are usually of secondary importance, and are neglected here.

The diagram in Figure 4 provides a representation of the shielding topology of the building. It illustrates the principal shielding surfaces presented to the external EM energy.

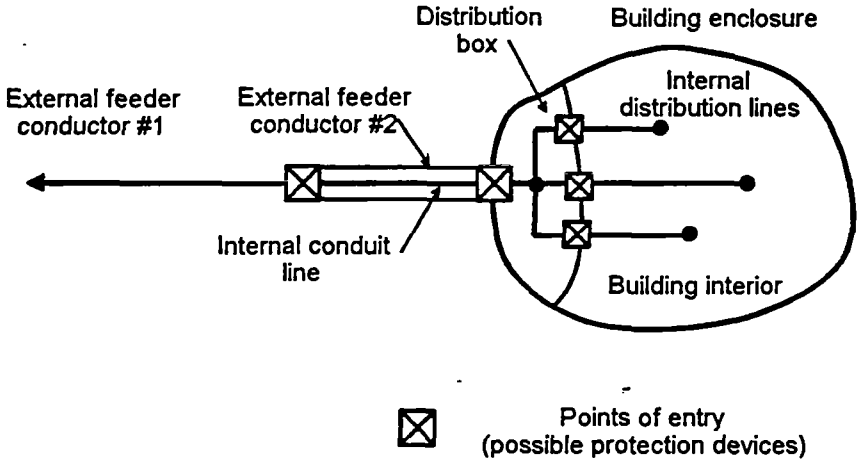

Figure 4. System topology.

6.3 INTERACTION SEQUENCE DIAGRAM

The interaction sequence diagram (ISD) is related to the topological diagram, in that it illustrates the paths along which EM energy propagates from the outside to the inside of the system, the penetration points in the shielding barriers, and the interrelations between the paths. For the system under consideration in this example, Figure 5 illustrates the ISD.

From this diagram is possible to estimate signal strengths at internal observation locations of interest, due to an external EM source. Furthermore, it can be used to identify the requirements for possible protection devices that might be placed at the points of entry (POE) locations.

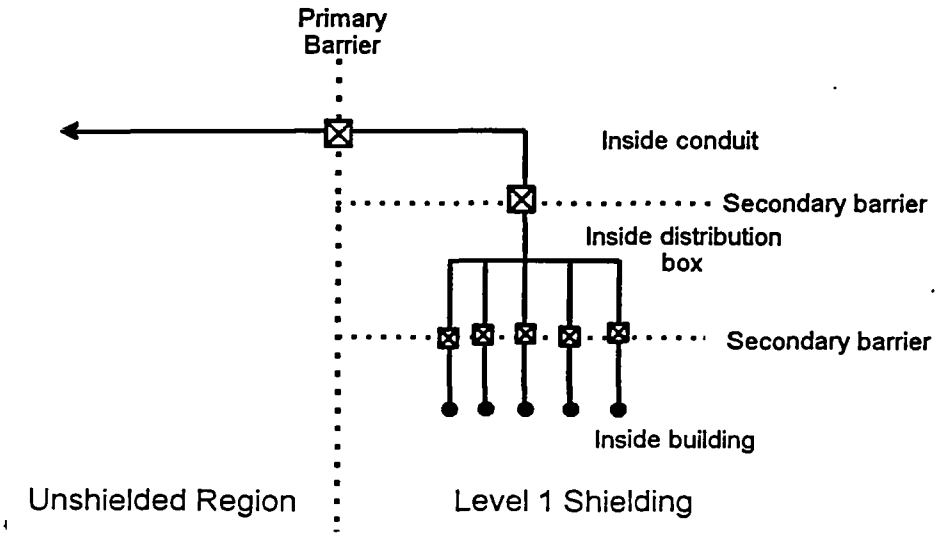

Figure 5. The interaction sequence diagram

6.4 SYSTEM MODEL

From the interaction sequence diagram, it is possible to develop a more detailed system model for calculating the propagation and penetration of energy along the network. This problem is modeled by an interconnection of transmission lines, as shown in Figure 6 below.

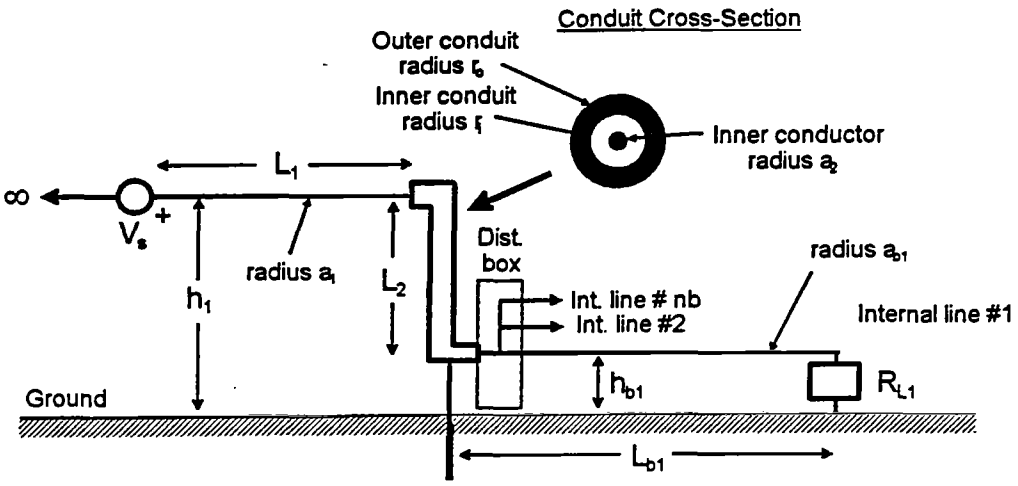

Figure 6. A transmission line model for the interaction path.

The first line is the external line #1 which represents the long line approaching the building. It is represented by an infinitely long conductor of height h_1 over the ground and a radius a_1. The voltage source exciting the line is located a distance L_1 away from the building end of the line.

The second line represents the external portion of the vertical conduit leading down to the circuit breaker box. The bottom end of this line is connected to the earth through a low footing resistance (which is assumed to be a short-circuit in this model). The length of this line is L_2, and the conduit has an outer radius given by r_o.

Line #3 is comprised of the internal portion of the conduit line, which has the coaxial cross-section shown in the figure. Its length is also L_2 and the two radii of the coaxial cross-section are r_i and a_2. This line conducts the external energy to the interior of the distribution box where it flows onto *nb* individual feeder lines distributed into the building interior.

Each of these internal lines is assumed to be described by its length L, height h, radius a and load resistance, R_L, as shown in the figure.

6.5 CIRCUIT DIAGRAM

The interconnection of transmission lines developed in the system model can be represented as a circuit model as shown in this figure. This permits the analysis of the voltage response at one of the internal transmission line loads. This analysis involves collapsing each of the lines down to a Thévenin equivalent circuit and then combining these circuits to compute the desired load response at a user-selected internal load resistance.

Any one of the *nb* internal loads may be selected for the calculation. The responses of interest that may be computed at the load include the transient voltage

waveform at the load, the peak maximum and minimum values of the load voltage, and the energy delivered to the load.

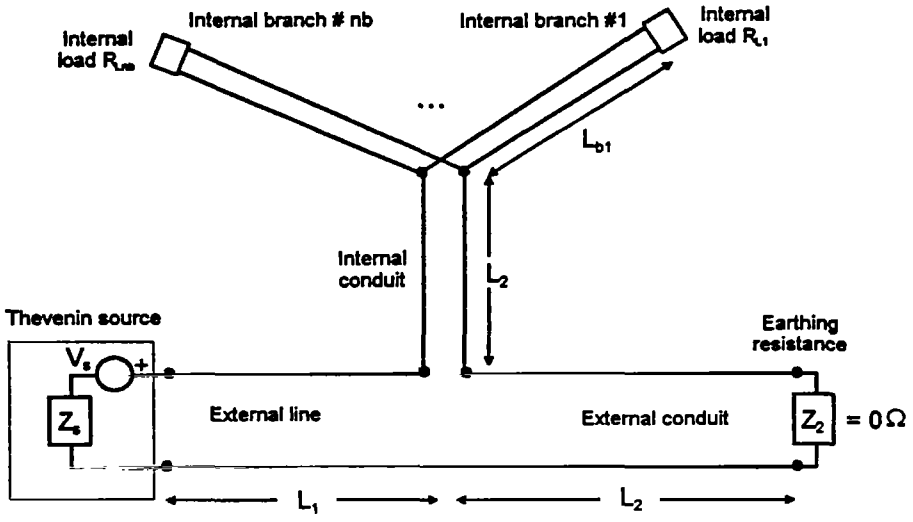

Figure 7. Circuit model for the transmission line network.

7. MODELING DETAILS

7.1 THE TRANSMISSION LINE MODEL

The basis for the model used in the calculations is the transmission line model shown in Figure 7. The choice of a transmission line type of model stems from past successful work with such models in lower-frequency problems, involving NEMP excitations, as well as recent work showing that transmission line models can be generalized in order to treat higher frequency problems.

The key element of the model is the representation of an end-fed transmission line of length L by a lumped equivalent circuit, as illustrated in Figure 8. For this line, it is assumed that it is described by a frequency dependent characteristic impedance, $Z_c(\omega)$, and a propagation constant $\gamma(\omega)$. Details of these parameters will be discussed later. Using the BLT equation for this transmission line[23], it can be shown that the open circuit voltage source, V_{oc} and the input impedance, Z_{in}, have the following expressions:

$$V_{oc}(\omega) = e^{-\gamma L}\frac{(1-\rho)}{\left(1-\rho e^{-2\gamma L}\right)}V_s(\omega) \tag{13}$$

$$Z_{in}(\omega) = \frac{1+\rho e^{-2\gamma L}}{1-\rho e^{-2\gamma L}}Z_c(\omega) \tag{14}$$

where ρ is the frequency dependent voltage reflection coefficient defined as

$$\rho(\omega) = \frac{Z_s(\omega)-Z_c(\omega)}{Z_s(\omega)+Z_c(\omega)}. \tag{15}$$

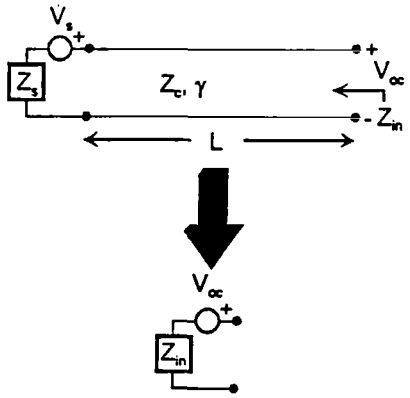

Figure 8. Representation of a single transmission line section by an equivalent Thévenin circuit.

---

[23] Tesche, F. M., "Plane Wave Coupling to Cables", Chapter 4 in Part II of *Handbook of Electromagnetic Compatibility*, R. Perez, ed., Academic Press, 1995.

This equivalent circuit representation of a transmission line section can be used to analyze the network shown in Figure 7 by applying it to successive branches and combining equivalent circuits in series or in parallel as needed. This procedure is illustrated in Figure 9, in which the external lines are first collapsed into two parallel equivalent circuits at the input of the coaxial line, (part *a* of the figure). These circuits are combined in series and then transformed to the end of the coaxial line (part *b* of the figure). The other internal branches are also collapsed and added in parallel, resulting in the circuit in part *c*. Then, this final transmission line circuit is collapsed down to the single lumped circuit shown in part *d*. The load voltage response is then calculated from simple circuit theory as

$$V_L(\omega) = \frac{Z_L(\omega)}{Z''''_{in}(\omega) + Z_L(\omega)} V''''_{oc}(\omega) \tag{16}$$

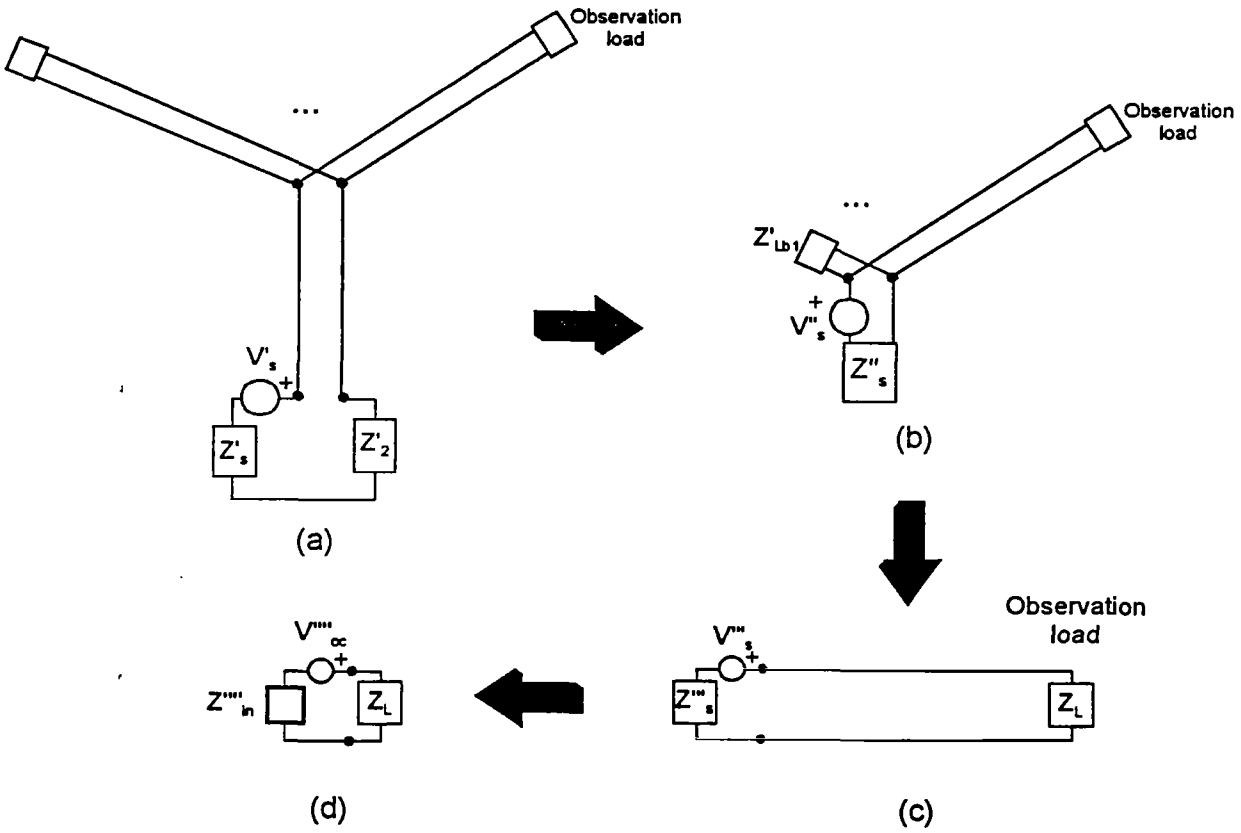

Figure 9. Analysis procedure for calculating the load response for the network in Figure 7.

7.1.1 The External Line Parallel to the Groundplane

For the model of the conductors of the system, there are several different classes of transmission lines used. Both inside and outside the facility, some of the lines can be viewed as a long conductor of radius a and parallel to a reference (ground) conductor at a height h. In the application of transmission line theory as described in the preceding section, it is usually required that the separation of two conducting wires be small compared with the wavelength (i.e., $h << \lambda$). However, recent work by Neff[24] and Tesche[25] suggest that the analysis can be extended to higher frequencies by using EM scattering theory to derive the per-unit-length impedance Z' and admittance Y' elements of the transmission line. Effectively, this implies that the propagation of EM energy along the conductors behaves like a TEM wave with its behavior being determined by the Telegrapher's equations, but that the characteristic impedance of the line is determined from an EM scattering problem.

Using this scattering theory approach, the propagation of energy along the line is close to be that of a wave in free-space:

$$\gamma(\omega) \approx j\omega / c, \tag{17}$$

and the characteristic impedance Z_c of a line of radius a and height h over a perfect conductor is expressed as

$$Z_c(\omega) = \sqrt{Z'/Y'} \approx \frac{Z_o}{4j}\left[H_0^{(2)}(ka) - H_0^{(2)}(2kh)\right], \tag{18}$$

where Z_o = 377 Ω is the characteristic impedance of free-space and $H_0^{(2)}()$ denotes the cylindrical Hankel function of the second kind. This last expression comes from the expressions given in ref.[25] for the per-unit-length line parameters obtained from scattering theory.

Simple transmission line theory provides the low-frequency characteristic impedance of the same line as

$$Z_c = \frac{Z_o}{2\pi}\ln\left(\frac{2h}{a}\right), \tag{19}$$

which is valid for $h << \lambda$. Figure 10 presents a comparison of the characteristic impedance magnitudes for a wire with height h = 1m over a prefect conductor, and with a radius a =

---

[24] Neff., H. P., Jr., and D. A. Reed, "The Effect of Secondary Scattering on the Induced Current in a Long Wire over an Imperfect Ground from an Incident EMP," *IEEE Trans. AP*, Vol 37, No.12, Dec. 1899, and private communication with the author.

[25] Tesche, F. M., "Comparison of the Transmission Line and Scattering Models for Computing the HEMP Response of Overhead Cables", *IEEE Trans. EMC*, Vol. 34, No. 2, May, 1992.

0. 5 cm, as calculated for the high frequency (scattering) model and for the low frequency (transmission line model). Note that these parameters are almost identical, as long at the condition $h << \lambda$ is maintained. However, as the frequency is increased and the line height becomes comparable to or exceeds the wavelength, the two impedances become quite different, as indicated in Figure 11. This illustrates one of the reasons why the low frequency transmission line theory begins to become inaccurate at higher frequencies.

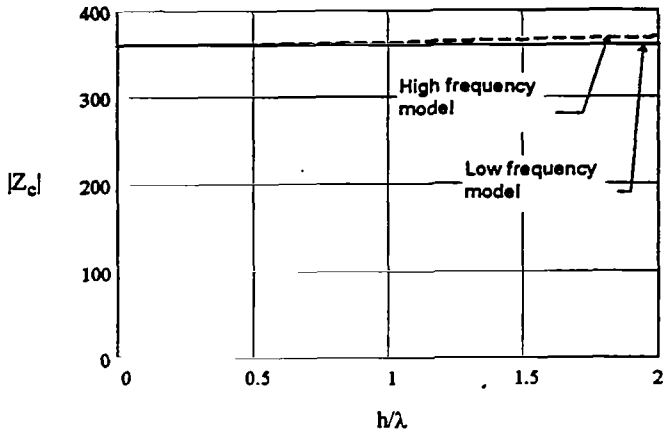

Figure 10. Comparison of the characteristic impedance for a line with h = 1m and a = 0. 5 cm for the high frequency (scattering) model and the low frequency (transmission line model).

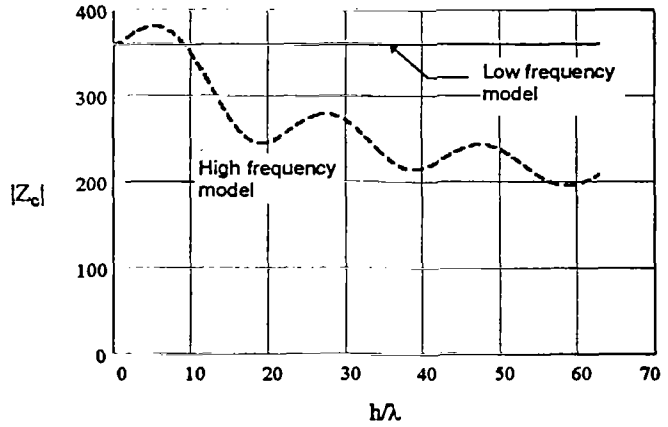

Figure 11. Comparison of the characteristic impedances of Figure 10 at higher frequencies.

As an example of the differences in the line responses when the scattering-derived parameters are used, consider the case of a single section of transmission line of Figure 8 with a line length L = 5 m and h = 1 m and a = 0.5 cm. Assuming that the load impedance is Z_s = 100 Ω (with no voltage source for this example), Figure 12 presents the input impedance magnitude at the open end of the line as a function of frequency. Notice that at

low frequencies, there is a good agreement between the two, but at high frequencies, there is a substantial deviation of the results.

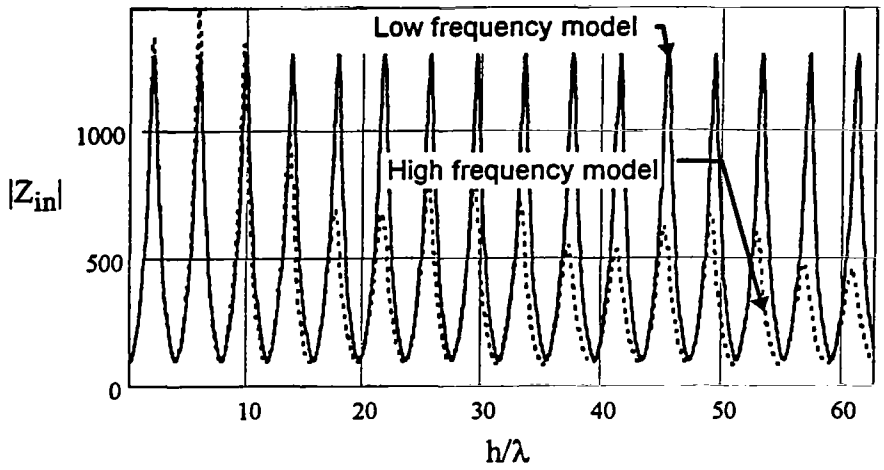

Figure 12. Example of the input impedance for a line with $L = 5$ m, $h = 1$ m, $a = 0.5$ cm and termination impedance of 100 Ω for the two different analyses.

Because the scattering results are based on a high-frequency solution to Maxwell's equations, they more accurately represent the actual behavior of the fields bound to the line. However, it is important to realize that in this model the presence of higher-order modes on the conductor have been omitted. These may contribute to the fields in the vicinity of the wire, and a detailed study of these modes in the context of HPM analysis appears not to have been done. Thus, this subject remains for future work.

7.1.2 The Vertical Transmission Line Section

The vertical transmission line section (i.e., the conduit exterior) appears much like a vertical antenna, on which current and charge propagate at the speed of light. Approximations to this type of problem are described by Schelkunoff[26], and this involves viewing the vertical section as a very thin biconical antenna of length L, cone half-angle ψ and average radius a. This structure has a characteristic impedance given by

$$Z_c = \frac{Z_o}{2\pi}\ln\left(\cot(\psi/2)\right) \approx \frac{Z_o}{2\pi}\ln(2L/a). \qquad (20)$$

Thus, using this expression and the propagation constant given in Eq.(17) permits the vertical conduit section to be treated like a transmission line. This approach has been

[26] Schelkunoff, S.I., and H. T. Friis, *Antenna: Theory and Practice*. John Wiley & Sons, 1952, p 426.

used by Degaque[27] and Tesche[28] for the very early-time modeling of transmission lines with vertical sections, with good results.

7.1.3 The Coaxial Line

For the coaxial region within the conduit, the usual TEM mode of propagation is valid as long as the conduit cross-section is electrically small. For cross-sections on the order of several cm, which are typical for cable routes, the transmission line model will be valid for frequencies up to a few GHz.

For these cases, the line impedance is given by the simple expression

$$Z_c = \frac{Z_o}{2\pi} \ln \frac{r_i}{a} \tag{21}$$

where r_i is the interior radius of the conduit shield and a is the radius of the internal wire within the conduit. As before, Eq.(17) is used for the propagation constant of the cable.

---

[27] Degaque, P. and J. Hamelin, *Electromagnetic Compatibility*, Oxford Press, 1993.

[28] Tesche, F. M. and B. R. Brandli, "Observations on the Adequacy of Transmission Line Coupling Models for Long Overhead Cables", *Proceedings of the International Symposium EMC'94 ROMA*, Sept. 13-16, Rome.

8. COMPUTED RESPONSES

The system interaction model discussed above has been implemented in a computer code called SWNET[29], and this has been used to conduct a limited analysis of a hypothetical system to illustrate some of the issues discussed in the previous sections. With reference to Figure 6, the following hypothetical system parameters have been chosen:

External Line #1:	$L_1 = 10$ m
	$h_1 = 3$ m
	$a_1 = 0.01$ m
External Line #2	$L_2 = 2.5$ m
(and coax)	$h_2 = 2.5$ m
	$r_o = 0.05$ m
	$r_i = 0.04$ m
	$a_2 = 0.01$ m
Internal Line #1	$H_B(1) = 20$ m
	$h_B(1) = 0.5$ m
	$a_B(1) = 0.01$ m
	$R_L(1) = 50\ \Omega$

Note that this is a very simple example, using only one internal transmission line, which is the observation line.

For this particular example, we will assume that the excitation voltage source is a simple exponentially damped sine wave given by

$$V_s(t) = V_o \Gamma\left(e^{-\alpha t} \sin(2\pi f_o t)\right) \qquad (22)$$

with V_o = 1 v, α = 0.1 (1/ns), f_o = 100 MHz, and Γ is chosen so that the peak value of $V_s(t)$ is equal to V_o. This results in the fast-rising waveform pulse shown in Figure 13, with a rise time of a bit more that 1 ns.

[29] "User's Manual for the Single Wire Network Program (SWNET)", prepared by F. M. Tesche, February 20, 1996.

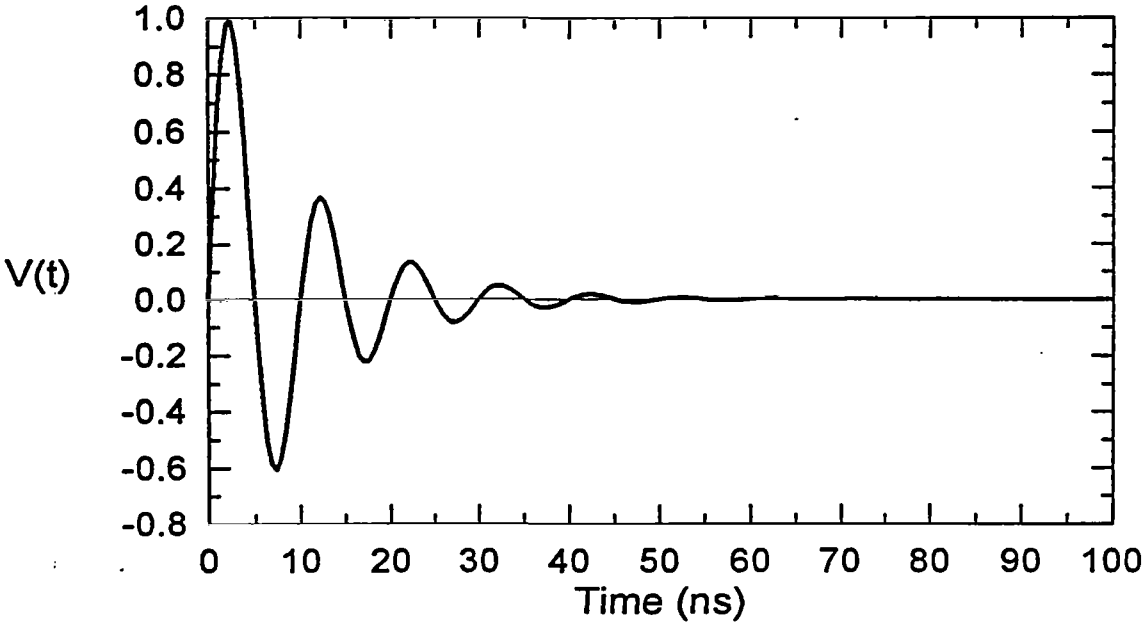

Figure 13. Excitation waveform $V_s(t)$ for sample calculation.

The Fourier spectrum of this waveform is expected to have a peak at the carrier frequency f_o, but it will also have significant energy away from this frequency, since the waveform is not purely sinusoidal. Figure 14 presents the calculated spectral magnitude for this excitation function.

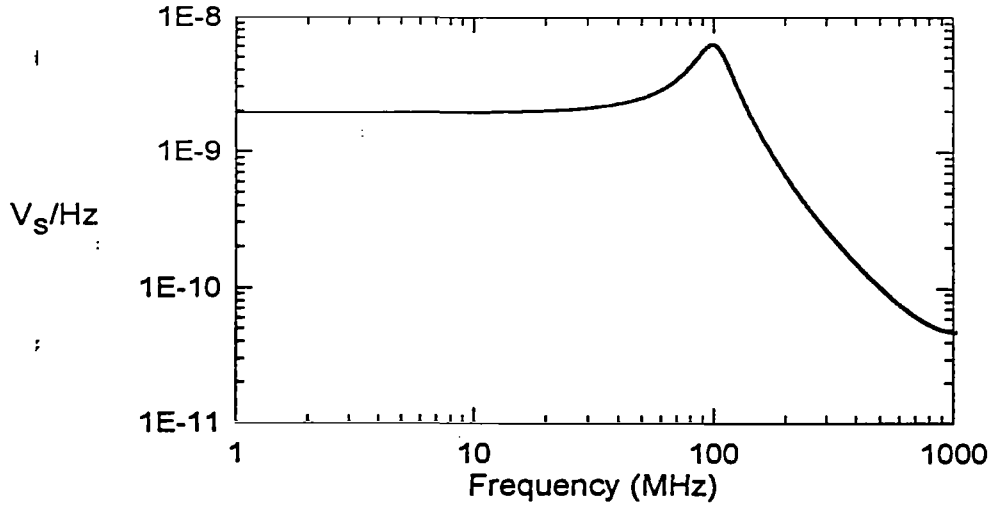

Figure 14. Spectral magnitude of the damped sine excitation function.

8.1 SYSTEM RESPONSES

8.1.1 Baseline Responses

For the given transient excitation of the sample problem, a calculation of the internal response was performed, and the resulting waveform is illustrated in Figure 15. Calculation of the response scalars provide the following values: V_{max} = 0.072 V, V_{min} = -0.048 V, and *Energy* = 0.87 × 10^{-12} Joules.

This waveform exhibits several interesting features. First, its amplitude is considerably lower than the 1 volt initially applied to the conductor. The attenuation is due to impedance mismatching at the transmission line junctions. Furthermore, there are several reflections of the initial waveform which occur from the "ringing" of energy on the network. Although the secondary pulses generally do not affect the peak voltages of the response, they do have an effect on the load energy.

Figure 17 presents a comparison of the spectrum of the computed load voltage and the driving voltage spectrum. The overall attenuation of the spectrum is noted, but also, we see that there are many peaks and nulls in the response spectrum introduced by the internal ringing on the network.

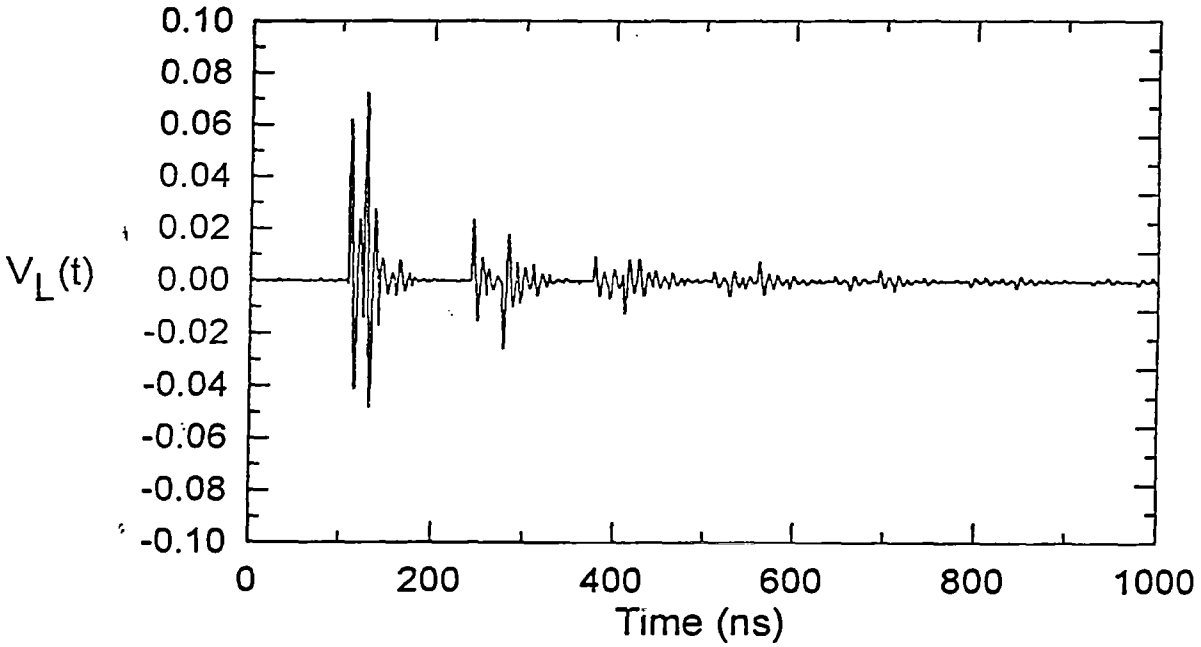

Figure 15. Transient load voltage at the internal load.

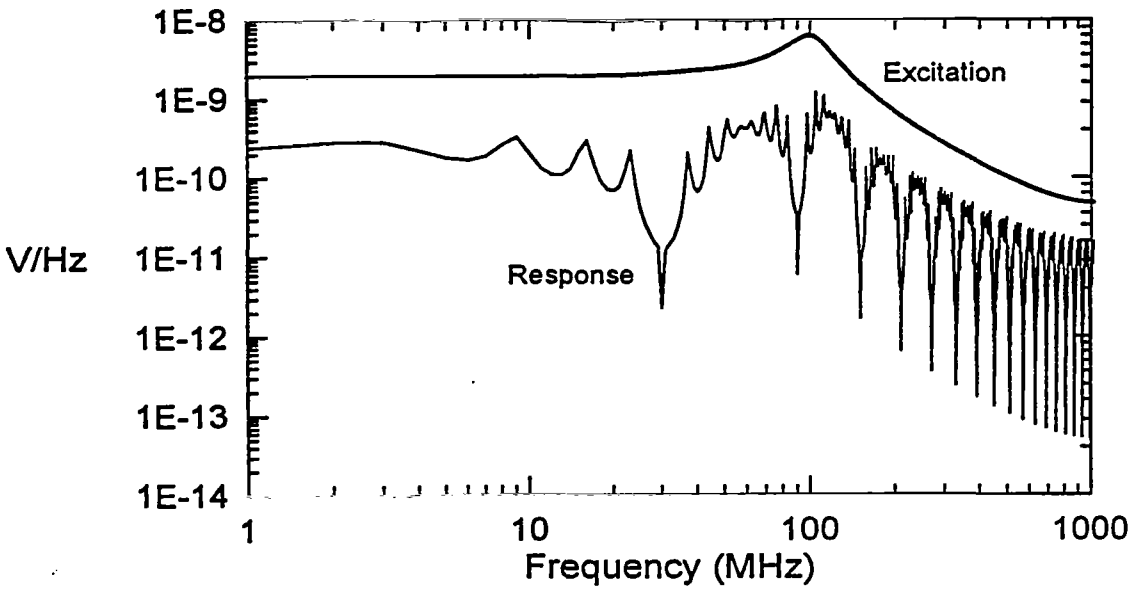

Figure 16. Comparison of the load voltage spectrum and the excitation spectrum.

8.1.2 Elasticities

Using the SWNET code, it is also possible to compute the elasticities of the response scalars as discussed in Section 3.2. These quantities are presented in Figure 17 for the sample problem. Note that the 3 scalar observables are all plotted on the same plot, with both positive and negative directions being indicates. Plotted along the x-axis are the names of the various parameters for which the elasticities are computed. Note that the lengths of the lines appear to be most important in determining these response characteristics.

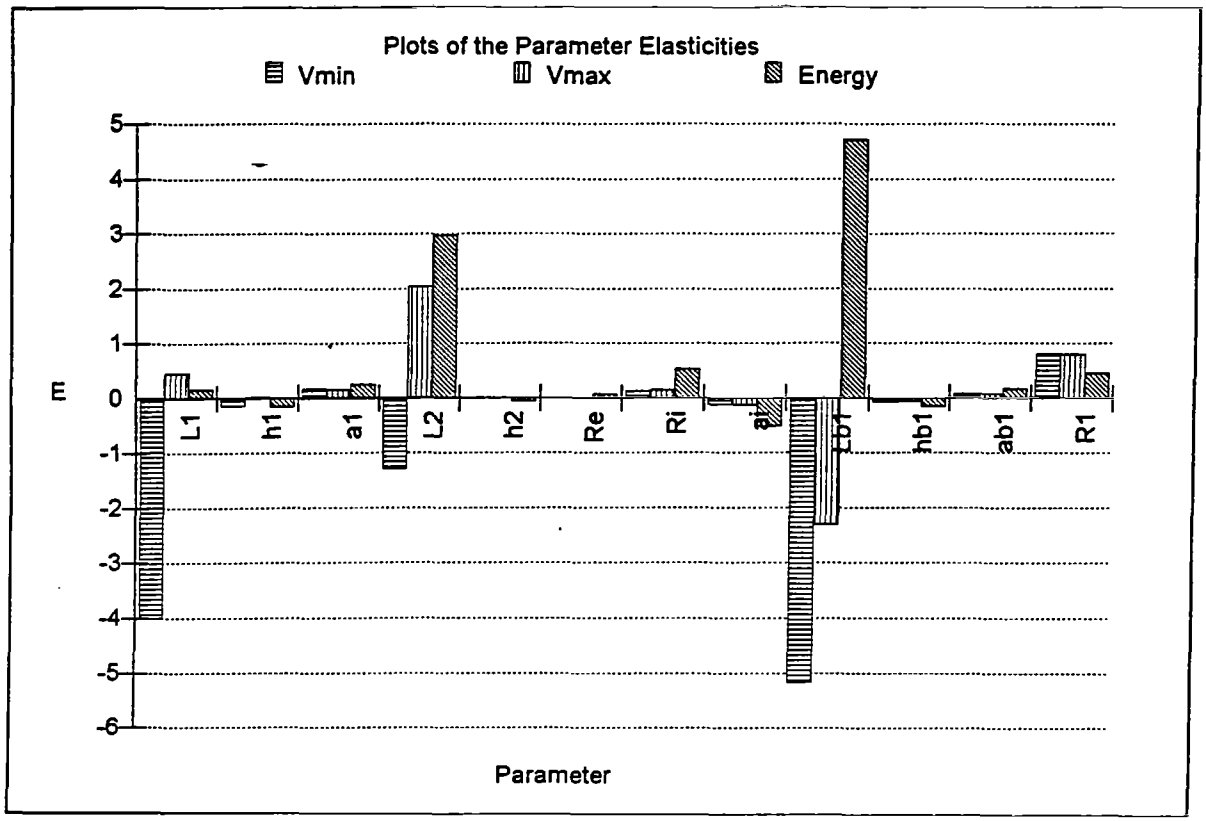

Figure 17. Elasticities for the scalar parameters.

8.1.3 Difference Waveforms

In the same calculation of the response elasticities, the SWNET program computes the response waveform differences for a 1% change in each of the parameter values. Thus, for the problem under discussion here, there are a total of 12 separate waveforms to study. Shown here are only 3, one for a change in the line #1 length, L_1, another for a change in the height parameter h_2 which pertains to the average height of the conduit over the ground, and the final waveform which illustrates the effect of changing the radius of the internal line radius, a_{b1}. These waveforms are shown in Figure 18, Figure 19, and Figure 20, respectively.

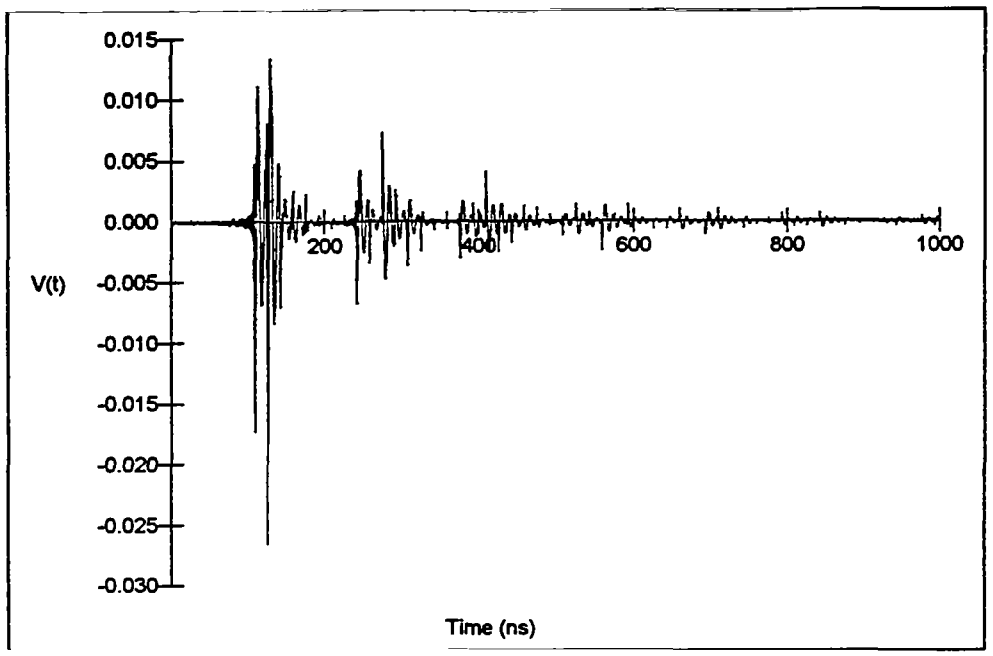

Figure 18. Plot of the difference in the load voltage response for a 1% change in the value of the external line length, L_1.

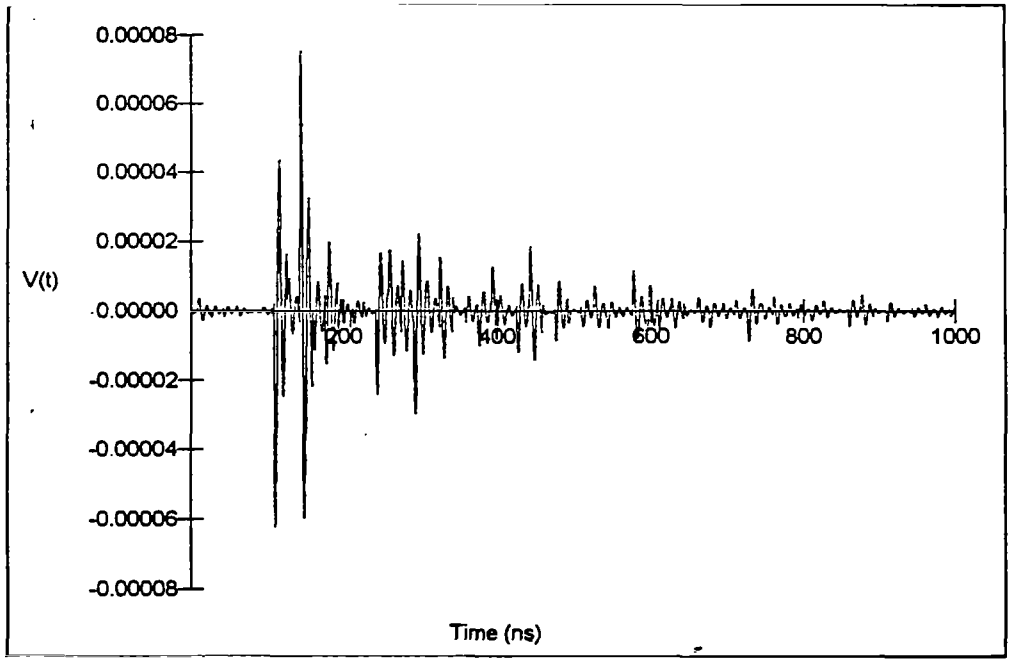

Figure 19. Plot of the difference in the load voltage response for a 1% change in the value of h_2.

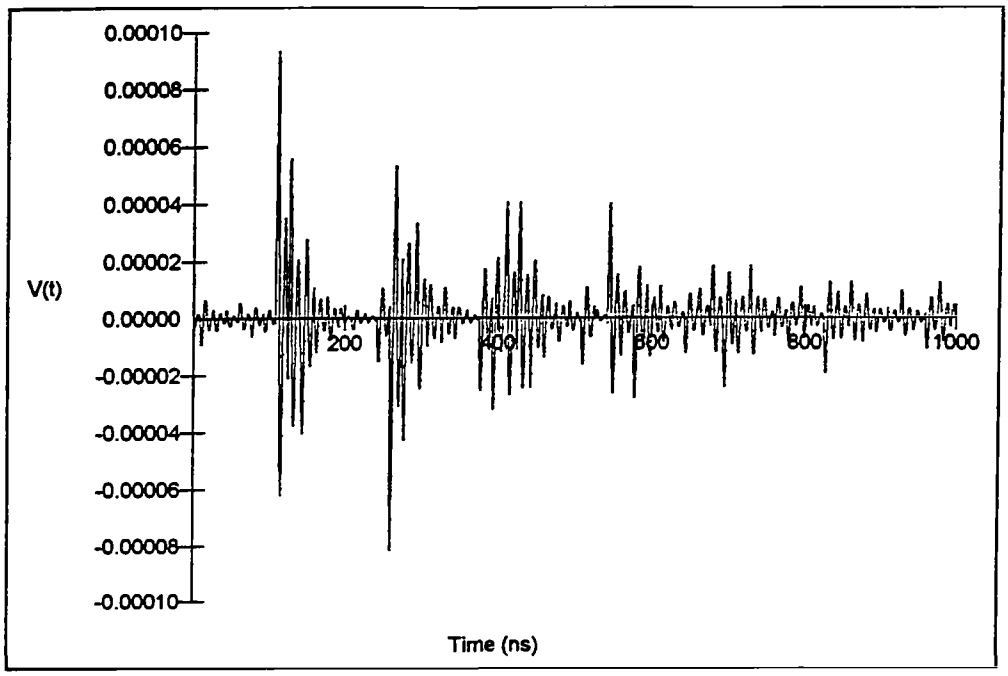

Figure 20. Plot of the difference in the load voltage response for a 1% change in the value of the internal line radius, a_{bl}.

8.2 STATISTICAL RESPONSES

Performing the Monte Carlo calculations as described in Section 4.2 permits the best understanding of how the response quantities of the system might vary in a real situation. In doing this, it is necessary to be able to quantify the uncertainties in the input parameters of the problem, as discussed in Section 4.1. In the present study, we have assumed that each parameter is described by the Gaussian distribution of Eq.(6), with a standard deviation of 10% of the nominal mean value of the parameter. Thus, we assume that $\sigma = 0.1\mu$. This is a rather large variation in the parameters, and in a real case, considerably smaller uncertainties might be possible. Of course, this depends on the nature of the problem and on the ability to measure it accurately.

Using the baseline data for the sample system previously given, the SWNET program was run to compute a total of $2^{14} = 16{,}384$ individual cases with random variations in the input data. (This is the largest number of cases that may be run at one time in the program, due to dimension limitations. The time for such a calculation was on the order of 6.8 hours on a 60 MHz Pentium computer.) The results of this calculation are presented in the next sections.

8.2.1 Probability Density Functions

The computed PDFs for the minimum and maximum load voltages and the energy delivered to the load are illustrated in Figure 21, Figure 22, and Figure 23, respectively. Notice that even though 16,384 cases were run, there still is a definite graininess in the

distribution. As a check of these calculations, we see that the peak values of the distributions occur very near the calculated scalar values for the baseline case of V_{max} = 0.072 V, V_{min} = -0.048 V, and *Energy* = 0.87×10^{-12} Joules.

Recall that these PDFs are normalized so that the total probability is unity. This accounts for the rather large values of P in Figure 23 for the energy, since the values of the energy along the abscissa are very small.

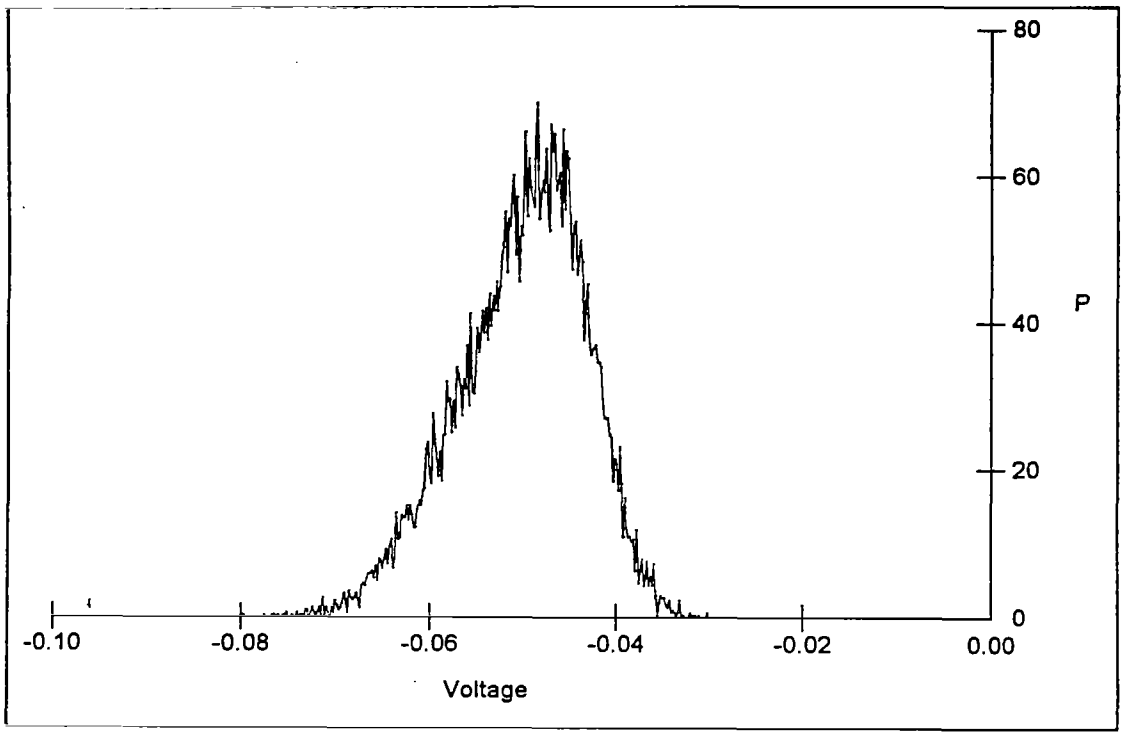

Figure 21. Probability density function for the peak negative load voltage.

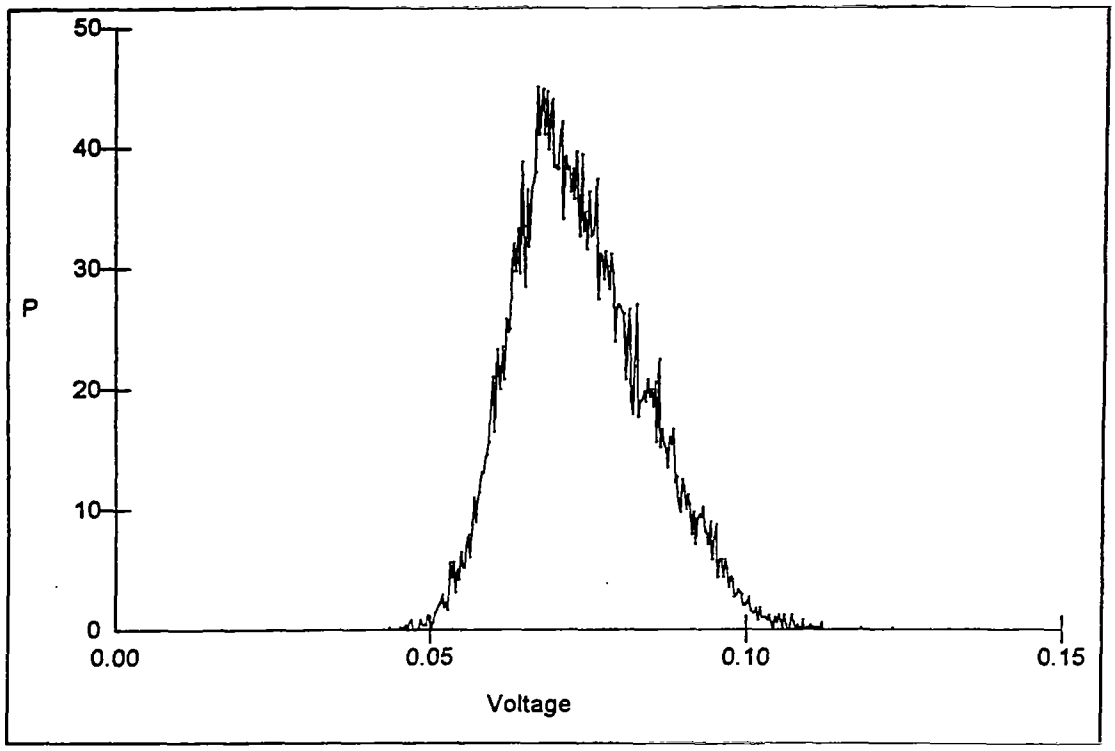

Figure 22. Probability density function for the peak positive load voltage.

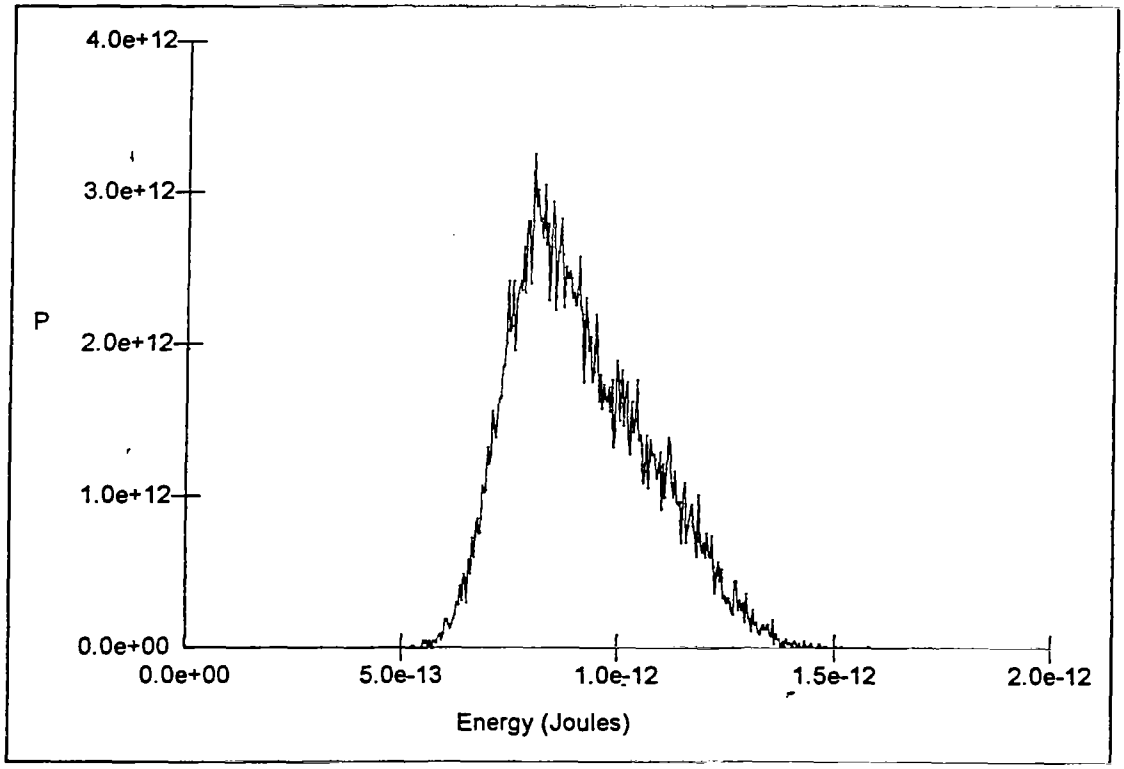

Figure 23. Probability density function for the energy delivered to the load.

8.2.2 Cumulative Probability Distribution

The computed CPDs for the observable quantities are presented in Figure 24, Figure 25, and Figure 26. Each of these figures show the probability of the observable quantity exceeding (in unsigned magnitude sense) the value specified along the abscissa of the plot.

Notice that these plots are very smooth in nature, due to the integration process mentioned earlier. Very good approximations to these curves can be obtained by running only a few hundred calculations. Hence, if only approximate CPDs are desired in a calculation, the required computer time can be considerable less than that needed for the 6,384 cases.

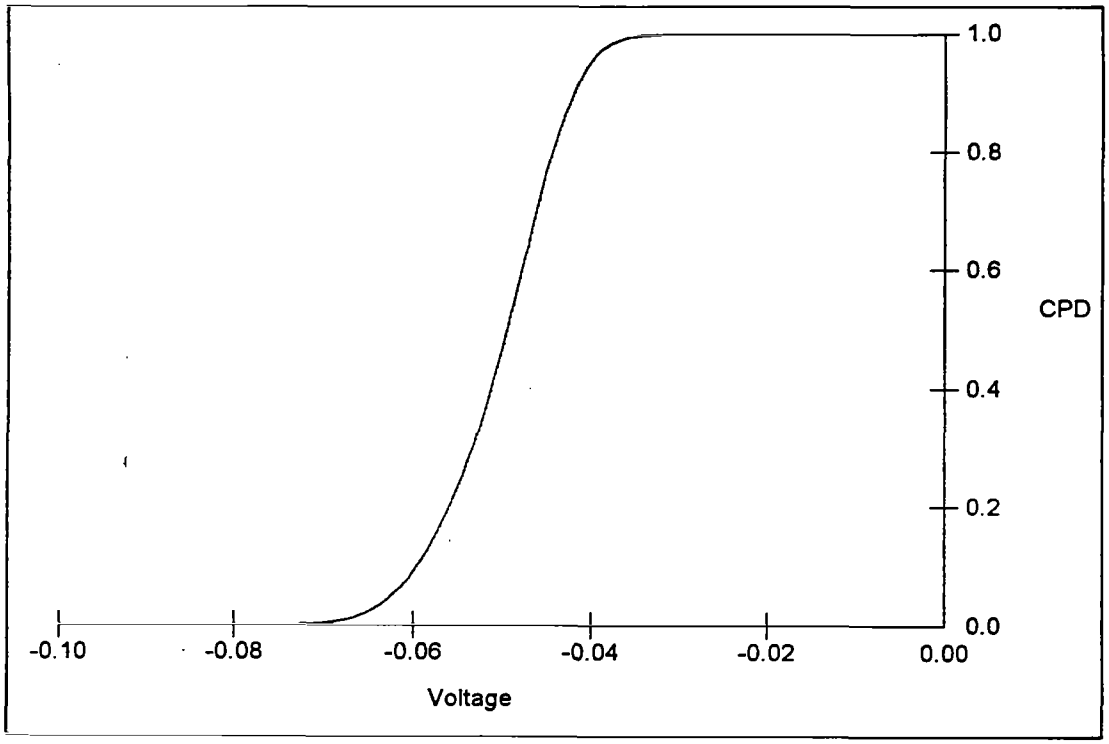

Figure 24. Cumulative probability distribution for the peak negative load voltage.

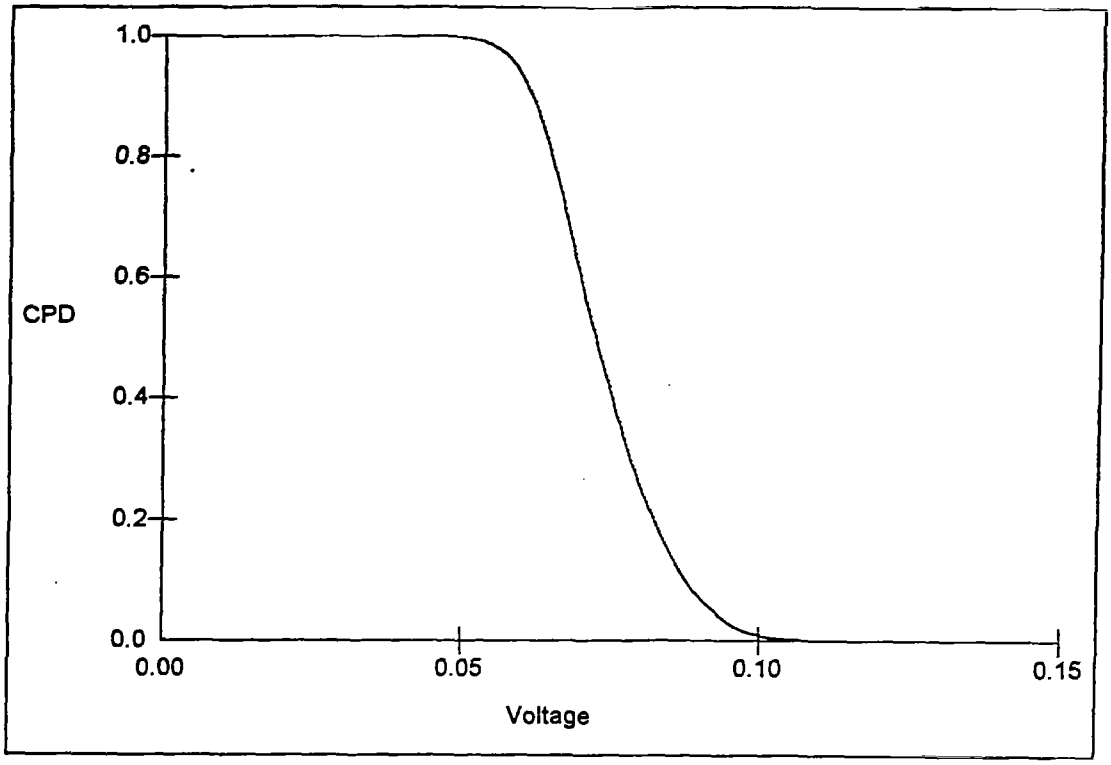

Figure 25. Cumulative probability distribution for the peak positive load voltage.

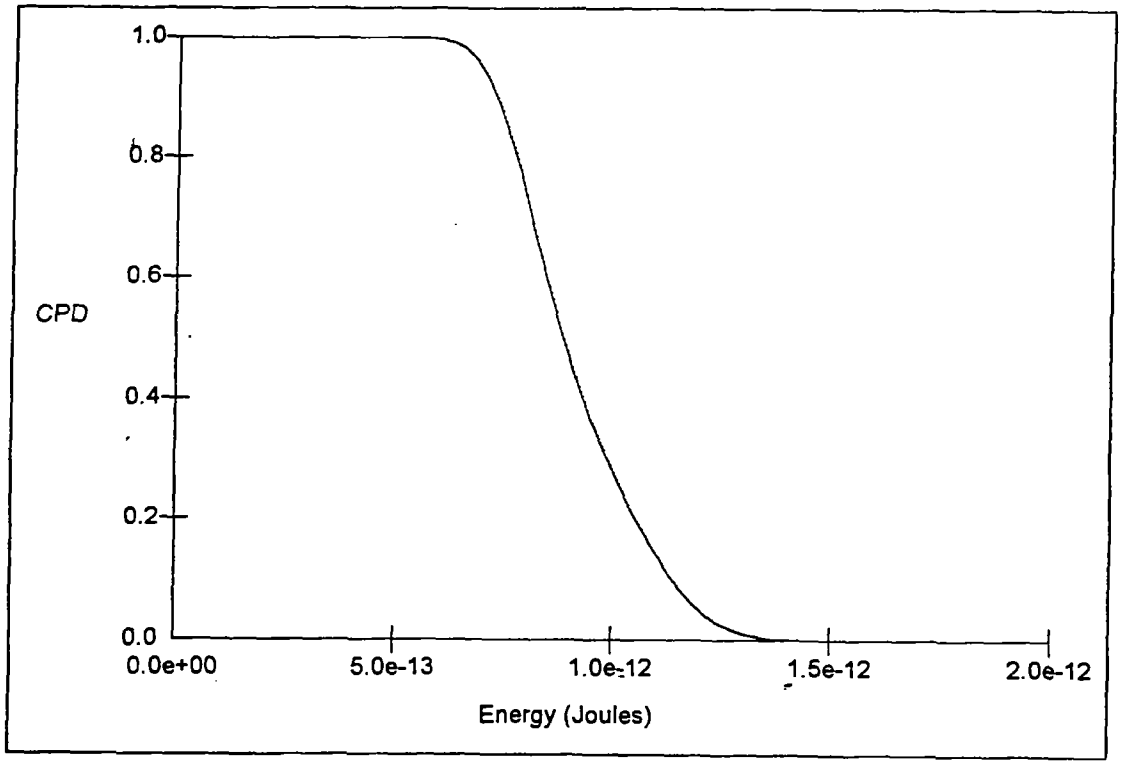

Figure 26. Cumulative probability distribution for the energy delivered to the load.

9. SUMMARY AND OBSERVATIONS

The purpose of this work has been twofold: to illustrate ways of using computational models to understand how electrically complex systems respond to EM energy, and to show how some previously-developed models for low frequencies ($f < 10$ MHz) can be extended to higher frequency problems.

What is suggested in the first area is familiar to anyone having a background in differential calculus—that the dependence of a function on many different variables can be understood by taking partial derivatives of the function with respect to each variable. In a complex system problem, this is not possible to do analytically, but with a computer model of the system, such derivatives can be evaluated numerically. Thus, a sensitivity study for the system can be performed. In addition, the repetitive use of such a numerical algorithm for computing system responses can be used in a Monte Carlo simulation for the distributions of selected responses.

Performing such an analysis for a real system may be more difficult that it first seems, however, in that it is necessary to have a reasonable probability distribution for the parameters of the problem. As mentioned in the text, a Gaussian distribution may not be the best choice, and additional work in understanding which of the analytical distributions are best for this purpose seems warranted. Moreover, the parameters needed to describe any chosen distribution must also be known. This implies that additional input data must be developed by the analyst, above and beyond that needed for a simple, deterministic analysis. However, as noted from the sample calculations here, the benefits of this type of calculation can be great, because the range of responses are given, not just the nominal value. This information is invaluable for system assessments and design.

In the second area of model extension for high frequency use, it is obvious that much work remains to be done. For example, the validation of the scattering formulation for the transmission line equations has been undertaken in ref.[23], but this has been done only for a limited range of frequencies. Quantifying how well these models work for frequencies when the line height approaches 20 to 100 λ would provide needed confidence in these high-frequency models. Other issues, such as the effects of radiation on the transmission line solutions, the changes of the propagation constant as higher frequencies and the possible effects of higher order modes on the line responses, are all interesting and deserve consideration. Consideration of these effects, however, was beyond the scope of the present study.

REFERENCES

1. Carter, J. M., and W. L. Curtis, "Common Mode Model Development for Complex Cable Systems", Boeing Company, AFWL-TR-74-60, 1974.

2. Ricketts, L. W., J. E. Bridges and J. Miletta, *EMP Radiation and Protective Techniques*, John Wiley and Sons, New York, 1976.

3. Baum, C. E., "How to Think About EMP Interaction", *Proceedings of the 1974 Spring FULMEN Meeting*, Kirtland AFB, April 1974.

4. Tesche, F. M., et. al., "Internal Interaction Analysis: Topological Concepts and Needed Model Improvements", Interaction Note Series, IN-248, October 1975.

5. Tesche, F. M., "Topological Concepts for Internal EMP Interaction," *IEEE Trans. AP*, Vol. AP-26, No. 1, January 1978.

6. Baum, C. E., "Electromagnetic Topology for the Analysis and Design of Complex Electromagnetic Systems", pp. 467-547 in *Fast Electrical and Optical Measurements*, Vol I, eds. I.E. Thompson and L.H. Luessem, Martinus Nijhoff, Dordrecht, 1986.

7. Vance, E. F., and W. Graf, "The Role of Shielding in Interference Control", *IEEE Trans. EMC*, Vol. 30, No.3, August, 1988.

8. Karlsson, T. "The Topological Concept of a Generalized Shield," AFWL Interaction Note 461, Kirtland AFB NM, January 1988.

9. Tesche, F. M, et. al., "Application of Topological Methods for Electromagnetic Hardening of the MX Horizontal Shelter System", LuTech, Inc. report prepared for Air Force Weapons Laboratory and Mission Research Corporation under Contract F29601-78-C-0082, January 1981.

10. Tesche, F. M., et. al., "Summary of Application of Topological Shielding Concepts to Various Aerospace Systems", LuTech, Inc. report prepared for Air Force Weapons Laboratory and Mission Research Corporation under Contract F29601-78-C-0082, February 1981

11. Tesche, F.M., "Introduction to Concepts of Electromagnetic Topology as Applied to EMP Interaction With Systems", NATO/AGARD Lecture Series Publication 144, *Interaction Between EMP, Lightning and Static Electricity with Aircraft and Missile Avionics Systems*, May 1986.

12. Longmire, C. L., private communication with the author, Mission Research Corp., 1980.

13. Parmantier, J. P., V. Gobin, and F. Issac, "Application of EM Topology on Complex Systems", *Proceedings of the 1993 IEEE EMC Symposium*, Dallas, TX. August 1993.

14. Parmantier, J. P., et. al. "An Application of the Electromagnetic Topology Theory to the EMPTAC Test-Bed Aircraft", Proceedings of the 6th FULMEN Meeting, Phillips Laboratory, November 29, 1993.

15. Baum C. E., F. M. Tesche, and T.K. Liu "On the Analysis of General Multiconductor Transmission Line Networks", EMP Interaction Notes, Note 350, November 1978.

16. Tesche, F. M, and T. K. Liu, "User Manual and Code Description for QV7TA: A General Multiconductor Transmission Line Analysis Code", LuTech, Inc., prepared under AFWL contract F29601-78-C-0002, August 1978.

17. Tesche, F. M., M. Ianoz, and T. Karlsson, *EMC Analysis Methods and Computational Models*, John Wiley and Sons, New York, in press.

18. Baum, C. E., "Norms and Eigenvector Norms", *Mathematics Notes*, Note 63, November 1979.

19. Thomas, G. B., *Calculus and Analytic Geometry*, Fourth ed., Addison-Wesley, Reading Mass, 1968,. p 255.

20. Morgan, M. A. and F. M. Tesche, "Basic Statistical Concepts for Analysis of Random Cable Coupling Problems," *IEEE Trans. AP*, Vol. AP-26, No. 1, January 1978.

21. Graham, W. R., and T. C. Mo, "Probability Distribution of CW Induced currents on Randomly Oriented Subresonant Loops and Wires", *IEEE Trans. AP*, Vol. AP-26, No. 1, January 1978.

22. Press, W. H., et. a., *Numerical Recipes*, Cambridge Press, New York, 1866, p. 203.

23. Tesche, F. M., "Plane Wave Coupling to Cables", Chapter 4 in Part II of *Handbook of Electromagnetic Compatibility*, R. Perez, ed., Academic Press, 1995.

24. Neff., H. P., Jr., and D. A. Reed, "The Effect of Secondary Scattering on the Induced Current in a Long Wire over an Imperfect Ground from an Incident EMP," *IEEE Trans. AP*, Vol 37, No.12, Dec. 1899, and private communication with the author.

25. Tesche, F. M., "Comparison of the Transmission Line and Scattering Models for Computing the HEMP Response of Overhead Cables", *IEEE Trans. EMC*, Vol. 34, No. 2, May, 1992.

26. Schelkunoff, S.I., and H. T. Friis, *Antenna: Theory and Practice*. John Wiley & Sons, 1952, p 426.

27. Degaque, P. and J. Hamelin, *Electromagnetic Compatibility*, Oxford Press, 1993.

28. Tesche, F. M. and B. R. Brandli, "Observations on the Adequacy of Transmission Line Coupling Models for Long Overhead Cables", *Proceedings of the International Symposium EMC '94 ROMA*, Sept. 13-16, Rome.

29. "User's Manual for the Single Wire Network Program (SWNET)", prepared by F. M. Tesche, February 20, 1996.